The Iranian Journal of Mechanical Engineering Transactions of ISME
Journal homepage: https://jmee.isme.ir/
Vol. 24, No. 2, 2023, pp. 6-41

Research Paper

DOI: https://doi.org/10.30506/jmee.2023.1972054.1302

Experimental Design by using Taguchi Method for Sensitivity Analysis of CuO/Deionized Water Nanofluid Properties

Seyed Amir Hossein Zamzamian[*]
Associate Professor

Faramarz Hormozi[†]
Associate Professor

Fahim Rahnamae Lashkami[‡]
M.Sc.

In this research, the thermal conductivity and viscosity of nanofluids has been investigated. So, the best response for the highest thermal conductivity and the lowest viscosity, respectively have been checked. For this purpose, the effect of simultaneous use of CuO/Deionized Water nanofluids to evaluate the thermal conductivity and dynamic viscosity is investigated and analyzed. The focus of the work is to investigate the influence of different transport phenomena parameters by using CuO nanoparticles dispersed in Deionized water. Given that the signal-to-noise ratio has calculated from the Larger–the better relationship, therefore, it has be concluded that the thermal conductivity of nanofluid is higher at higher volume fractions and temperatures. Finally, in this condition, volume fraction of 0.4% and temperature of 40°C will be more suitable. On the other hand, Because of the signal-to-noise ratio has calculated from the smaller-the better relationship, therefore, it has be concluded that the dynamic viscosity of nanofluid is lower at lower volume fractions and higher temperature. And also, the volume fraction of 0.1% and the temperature of 33.3°C will be more suitable.

Keywords: Sensitivity analysis, Nanofluid, Taguchi method, Thermal conductivity, Dynamic Viscosity

1 Introduction

Over the past decades working fluids based on type, and function in most of the production and operation processes have been involved where, depending on the application and the

[*]Corresponding Author, Associate Professor, Energy Department, Materials and Energy Research Center (MERC), Energy Department, Solar Energy Group, Karaj, Iran, azamzamian@merc.ac.ir
[†]Professor, Faculty of Chemical, Petroleum and Gas Engineering, Semnan University, Semnan, Iran, fhormozi@semnan.ac.ir
[‡]M.Sc., Faculty of Chemical, Petroleum and Gas Engineering, Semnan University, Semnan, Iran, frahnama@semnan.ac.ir

Received: 2022/11/05, Revised: 2023/05/08, Accepted: 2023/12/27

working conditions of the equipment, particular characteristics were required [1]. Diversity in methods and techniques has been observed so that attempts to describe the historical evolution of the transient hot-wire technique, employed today for the measurement of the thermal conductivity of fluids and solids over a wide range of conditions. Researches with a discussion of the areas of application where problems still exist, and a glimpse of the technique's future have been concluded [2].

Some experimental instrument manufacturers unfortunately by reducing accuracy, they cause to easiness and speed of operation, that's the issue in some conditions, produce incorrect data, which cannot be validated by standard reference data or certified reference materials. However, the best available techniques for the measurement of thermal properties of fluids, with special emphasis on transient methods and their application to ionic liquids, nanofluids, and molten salts have been critically reviewed [3]. A comprehensive overview by the need of finding a standard and normalize procedures, to measure thermal conductivity in thermal energy storage media, regardless the ultimate application have been outlined. Based on this review, the available and commercialized methods to measure thermal conductivity have been classified in two methods including: steady-state and transient as in Figure (1). Also steady-state conditions methods are included guarded hot plate and heat flow meter. On the other the transient conditions methods are in the followings: transient plane source, transient hot wire, laser flash apparatus, modulated DSC, 3ω method and thermocouple method [4]. Copper oxide nanoparticles of average size of 8 nm by a simple precipitation technique have been synthesized and the thermal properties of the suspensions have investigated.

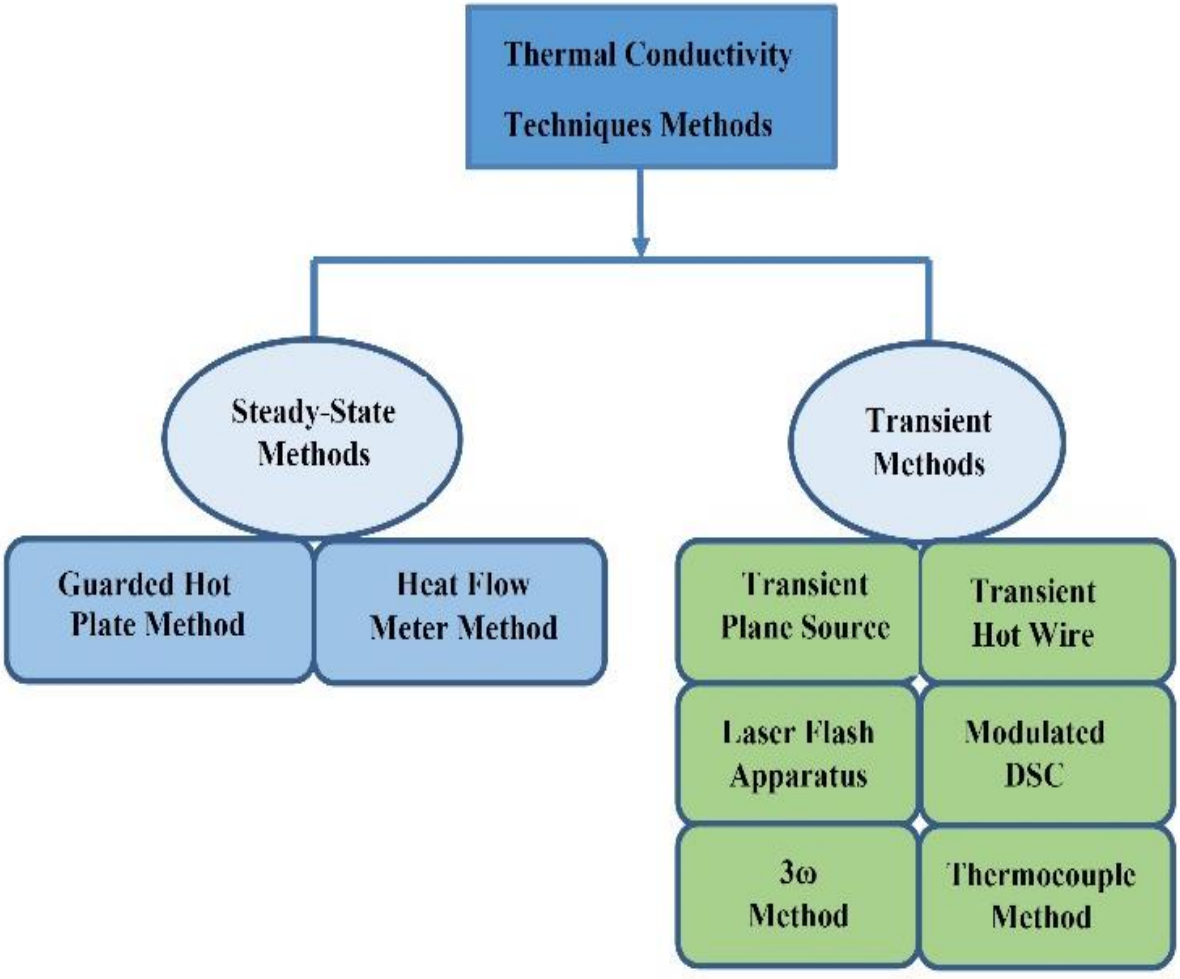

Figure 1 Types of classifications for the thermal conductivity measurement techniques

In this case nanofluids based on water and Ethylene Glycol with 1 vol.% Copper oxide NPs, the thermal conductivity enhancement has been observed by 31.6 and 54%, respectively. Therefore, the experimental results show that some of main factors such as: the NPs size, poly-dispersity, cluster size and the volume fraction of NPs, a significant influence on thermal conductivity have been had [5]. One important consideration is that NMs based on Carbon because of low density, compared with metal based ones have been had low density, better stability and dispersion. Anyway, in spite of its great potential, by more dispersion of nanoparticles can also it causes unsuitable side effects such as: sedimentation, agglomeration, increase of the viscosity and higher material cost [6, 7]. Actually, since a decade ago a rapid progress in research activities concerning enhancement in their thermal conductivity of nanofluids has been reported. But a review of research resources and available articles have showed that the increase in thermal conductivity of the nanofluids is completely unusual and odd [8]. From early research to recent decades, it has been observed that adding a small amount of NPs, produces a dramatic increase in thermal conductivity [9-12]. Even by the dispersion of NMs based on metal oxide and ceramic in the base fluids, its thermal conductivity have been substantially enhanced. Nanofluids formulated by aqueous based in such a way have found very stable and to investigate their heat transfer behavior under the natural convection conditions have been used [13-17]. Nanofluids have been increasingly investigated as shown in Figure (2) and since it has introduced in 1995 by Stephen Choi.

Some researchers have been indicated that the thermal conductivity of the nanoparticles was less relevant to increase the nanofluids heat transfer rates, but others suggest that nanoparticles with higher values of thermal conductivity may increase the heat transfer in the nanofluids [18]. However, on the other hand also the thermal conductivity of water-based nanofluids with copper and alumina nanoparticles have been compared. The heat transfer enhancement of two water-based nanofluids that under different the combined treatment with both the pH and chemical surfactant concentrations have been studied [19].

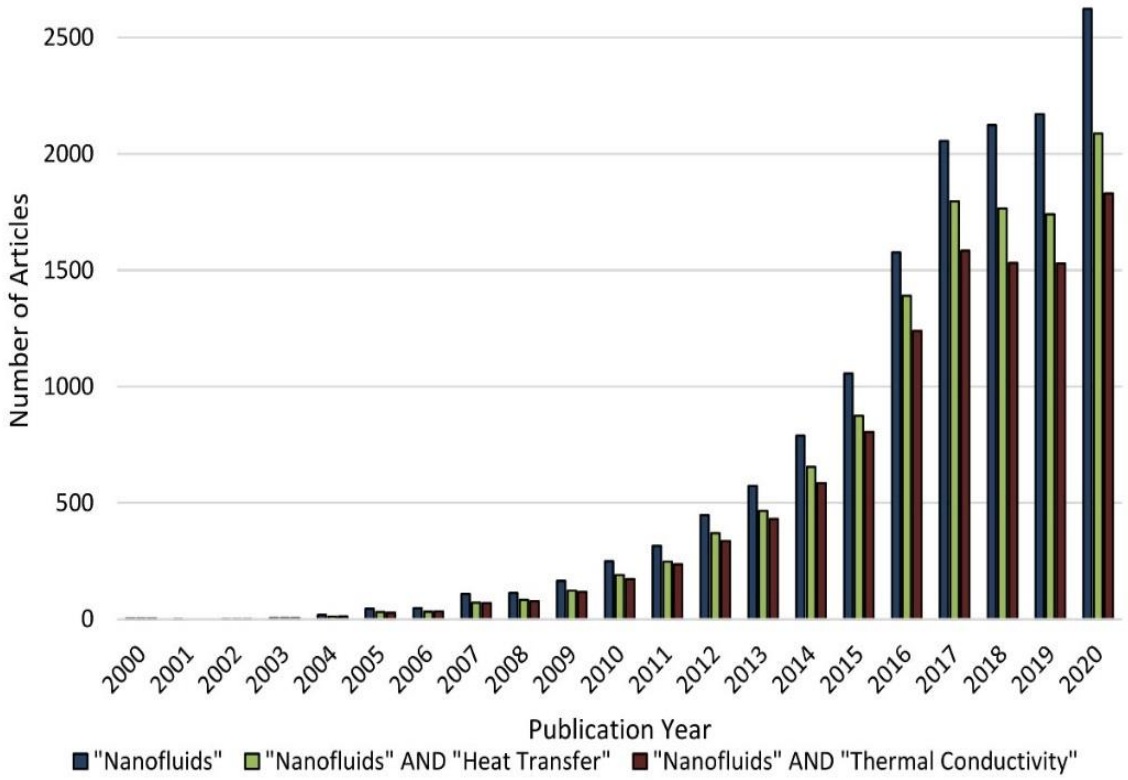

Figure 2 Column chart of scientific achievements in the Science Direct database that between January of 2000 and September of 2020 have been published

Table 1 Summary of empirical and experimental models of thermal conductivity coefficient of nanofluids

Researchers Name	Experimental Model	Main Factors and Results Reported
Xue and Xu [21]	$\left(1-\frac{\varphi}{\alpha}\right)\frac{k_{nf}-k_{bf}}{2k_{nf}+k_{bf}} + \frac{\varphi}{\alpha}\frac{(k_{nf}-k_i)(2k_i+k_p)-\alpha(k_p-k_i)(2k_i+k_{nf})}{(2k_{nf}+k_i)(2k_i+k_p)+2\alpha(k_p-k_i)(k_i-k_{nf})}=0$ $\alpha=\left[\frac{d_p}{d_p+2t_1}\right]$	An implicit model, thermal conductivity of nanoparticle and fluid, relative volume fraction, nanoparticle size and interfacial shell properties k_i and t_1 are as follows: the thermal conductivity and thickness of interfacial shell, respectively.
Hamilton and Crosser [22]	$k_{nf}=k_{bf}\left(\frac{k_{np}+(n-1)\,k_{bf}-\varphi(n-1)(k_{bf}-k_{np})}{k_{np}+(n-1)\,k_{bf}+\varphi(k_{bf}-k_{np})}\right)$	Particle shape , composition , thermal conductivities of base fluids and nanoparticles
Maxwell [23]	$k_{nf}=k_f\left(\frac{k_{np}+2\,k_{bf}+2\varphi(k_{np}-k_{bf})}{k_{np}+2\,k_{bf}-2\varphi(k_{np}-k_{bf})}\right)$	Thermal conductivity of base fluid and nanoparticles
Wasp [24]	$k_{nf}=k_{bf}\left(\frac{k_{np}+(n-1)\,k_{bf}-\varphi(n-1)(k_{bf}-k_{np})}{k_{np}+(n-1)\,k_{bf}+\varphi(k_{bf}-k_{np})}\right)$	Thermal conductivity of base fluid and nanoparticles and the spherical particles
Xuan [25]	$k_{nf}=k_{nfMaxwell}+\frac{1}{2}\rho_{np}Cp_{np}\varphi\sqrt{2D_B}$	Temperature and viscosity of base fluid, the average size and viscosity of the clusters of particles, and the brownian motion of particles
Koo and Kleinstreuer [26]	$k_{nf}=k_{nfMaxwell}+\frac{5\times10^4}{k_{bf}}\beta(\varphi)\rho_{bf}Cp_{bf}f(T,\varphi)\sqrt{\frac{k_BT}{\rho_{np}d_{np}}}$ $f(T,\varphi)=(-6.04\varphi+0.4705)T+(1722.3\varphi-134.63)$	Temperature and viscosity of the base fluid, volume fraction and type of nanoparticle, and molecular diffusion due to the brownian motion of particles
Xie, Fujii and Zhang [27]	$k_{nf}=1+3\Theta\varphi T+\frac{3\Theta^2\varphi^2T}{1-\Theta\varphi T}$	Volume Fraction ,Size and thickness of nanoparticles(or Nanolayer) , Thermal Conductivity Ratio of Nanoparticle to Base Fluid
Avsec and Oblak [28]	$k_{nf}=k_{bf}\left(\frac{k_{np}+(n-1)\,k_{bf}-(n-1)\varphi_{nf}(k_{np}-k_{bf})}{k_{np}+(n-1)\,k_{bf}+\varphi_{nf}(k_{np}-k_{bf})}\right)$ $\varphi_{nf}=\varphi\left(1+\frac{h}{r}\right)^3$	Layer thickness of the base fluid, thermal conductivities of base fluid and nanoparticle, (not related to the particle size and the interface between the particles)
Pak and Cho[29]	$k_{nf}=1+7.47\varphi$	Nanoparticle surface resistance, diameter and geometry
Yu and Choi [30]	$k_{nf}=k_{bf}\left[\frac{k_{pe}+2\,k_{bf}+2(k_{pe}-k_{bf})(1+\beta)^3\varphi}{k_{pe}+2\,k_{bf}-(k_{pe}-k_{bf})(1+\beta)^3\varphi}\right]$ $k_{pe}=k_{np}\left[\frac{[2(1-\gamma)+(1+\beta)^3(1+2\gamma)]\gamma}{-(1-\gamma)+(1+\beta)^3(1+2\gamma)}\right]$	Modified Maxwell model and nanolayer thickness
Wang et al. [31]	$k_{nf}=k_{bf}\left[1+\frac{\frac{3f_q(p)}{p_0}}{1-\frac{f_q(p)}{p_0}}\right]$	Nanolayer thickness, particle size, temperature, volume fraction, and adjacent particles interaction
Chandrasekar et al. [32]	**Model I:** $k_{nf}=k_{bf}\left[\left(\frac{Cp_{np,nf}}{Cp}\right)\left(\frac{\rho_{nf}}{\rho}\right)^{1.33}\left(\frac{M}{M_{nf}}\right)^{0.33}\right]$ **Model II:** $k_{nf}=k_{bf}\left[\frac{k_{np}+(n-1)\,k_{bf}+(n-1)(k_{np}-k_{bf})(1+\beta)^3\varphi}{k_{np}+(n-1)\,k_{bf}-(k_{np}-k_{bf})(1+\beta)^3\varphi}\right]$	This is including two models: Model I: For a wide range of particles by factors Fraction and size, and type of base fluid. Model II: Layer thickness ratio, particle shape, and brownian motion
Corcione [33]	$k_{nf}=1+4.4Re^{0.4}Pr^{0.66}\left(\frac{T}{T_{fre}}\right)^{10}\cdot\left(\frac{k_{np}}{k_{bf}}\right)^{0.03}\cdot\varphi^{0.66}$	For the following conditions: Temperature: 294–324 K Nanoparticle size: 10–150 nm Volume fraction : 0.002–0.9

In this way, according to the aforementioned explanations some of the empirical thermal conductivity prediction models and theoretical relations by using the referred researchers in the Table (1) have been presented. One of the basic topics of recent years in the field of nanofluids synthesis, preparation methods, thermal conductivity, and challenges of hybrid nanofluids have been, that also has been discussed. By precise screening of a broad range of studies in this field, thermal conductivity characteristic of Hybrid nanofluids than the normal nanofluids have been improved. But indeed results indicate that the selection of proper hybrid nanoparticles by a major challenge for preparing stable nanofluids, have been always accompanied. However, knowledge and deep understanding on these field in order to develop hybrid nanofluids for better thermal properties have been required [20]. Of course before implementing the nanofluids in every applications, preparation of stable suspension of nanofluids have been important, as better preparation will result in better performance. Hereof, the thermal conductivity of nanofluid prepared by the surfactant has increased and appreciably after 6 h of sonication is shown in Figure (3). Also the mechanism behind the ultrasonic duration time of thermal conductivity have been schematically denoted.

The effect of sonication duration time about 0−2 hours on the thermal conductivity of nanofluid based on Alumina have been experimentally investigated, and found that thermal conductivity has been nearly constant over a certain sonication time for all volume fractions(φ) [21]. On the other hand, the cluster size of nanofluids by increase in sonication duration time about 1–5 hours have been decreased. The thermal conductivity with the rise of temperature and sonication duration time have been increased [22]. An exhaustive critical analysis to the predictive that models currently available for the thermal conductivity of nanofluids based on CNT have been presented. For this purpose, the statistical experimental analysis of the different available models have been carried out and therefore to select specific nanofluid variables as control factors namely particle geometry, volume fraction, temperature and base fluid have provided [23]. By using commercial Dynamic Light Scatterin (DLS): Beckman Coulter N4 Plus or DLS measurements to estimate the size of Alumina nanoparticles as suspended in their carrier base fluids have been performed. The DLS technique also monitors the Brownian motion of particles have dispersed in a base fluids by illuminating the sample with a laser beam and detecting the scattered light [24].

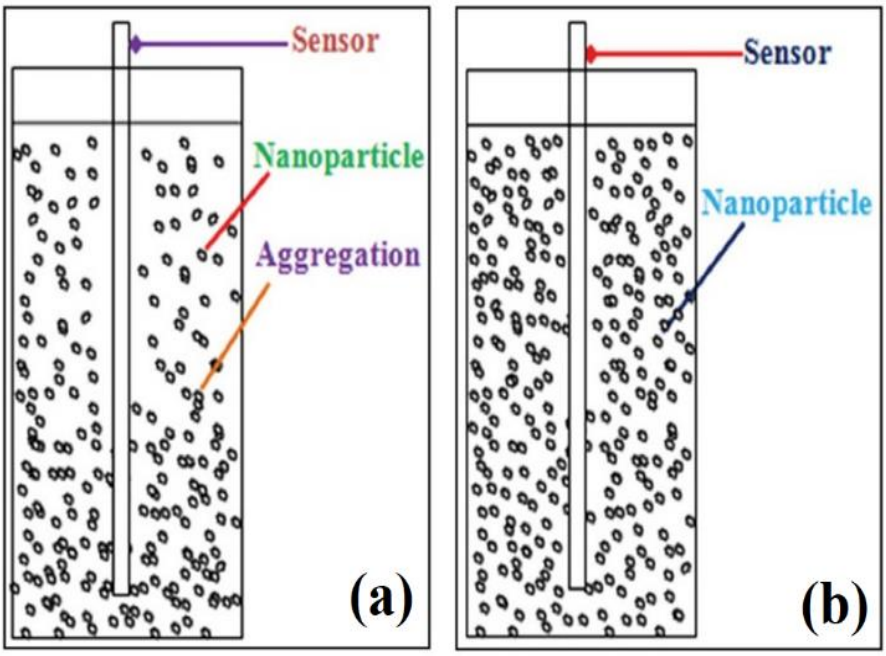

Figure 3 Effect of ultrasonic duration on thermal conductivity, **(a)** Lower ultrasonic; high aggregation and cluster, **(b)** Higher ultrasonic; no any aggregation

Table 2 The particle size measurements by DLS method for aqueous latex standard beads [24]

Specified Bead Size(nm)	The Size by DLS (nm)	Volume Fraction by DLS (%)
50	42.4 ± 8.1	100
Mixture of 50 nm/200 nm	44.2 ± 2.9	80.1
	177.9 ± 19.9	19.9

To assess the accuracy of the particle size measurements, two reference solutions containing latex beads of known diameters have been prepared. One solution with 50 nm beads and the other with a mixture by the ratio of 80:20, which have had 50 nm and 200 nm beads. Therefore the data in Table (2) have been in range 10–20% of the known diameters that for both solutions have been presented. It has been demonstrated that the DLS technique can provide reasonably accurate measurements of the size of nanoparticles [24]. On the other hand thermal conductivity of the ZnO–EG nanofluid by the size of 30–40^{nm} have increased from almost 21% to about 40% at the volume fraction 3.75% and as the sonication time 0−100 hours from 4 to 60 hours have been increased, and then for the sonication time of 100 hours, it has been decreased to around 35%. Therefore the effective thermal conductivity of the ZnO–EG nanofluids have increased by increasing the sonication time and has attained to maximum after the sonication time of almost 60 hours [25]. So due to this case the time of ultrasonic can disperse the particles more uniformly. When the ultrasonic time have been more than 3 hours, the value of thermal conductivity of nanofluids for the size of 50 nm, have tended to be constant. So that 3 hours of ultrasonic time is enough to disperse the nanoparticles of nanofluid [26]. By using sonication with high-powered pulses to improve the dispersion of particles in the preparation of nanofluids has been observed, and all nanofluids significant enhancement of thermal conductivity after sonication have been exhibited [27].

2 Materials and Method

2.1 Experimental apparatus details

In this study, copper oxide nanoparticles with size of 40 nm and deionized water as the base fluid to prepare nanofluids have been used. The physical and thermo-physical properties of the CuO nanoparticles have been presented in Table (3). The size of the particles by Transmission Electron Microscope (TEM) and the structural characteristics by X-ray diffraction spectrometry analysis have been determined as it's shown in Figure (4).

Table 3 Thermo-physical properties of CuO nanoparticles

Thermo-Physical Property	Value
Appearance	Black Powder
Morphology	irregular shapes
Particle Size (nm)	40
Purity	99%
Bulk density (kg/m^3)	790
True density (kg/m^3)	6400
SSA (m^2/g)	20
Thermal conductivity (W/m K)	32.9
Specific Heat Capacity(J/gr.K)	0.54

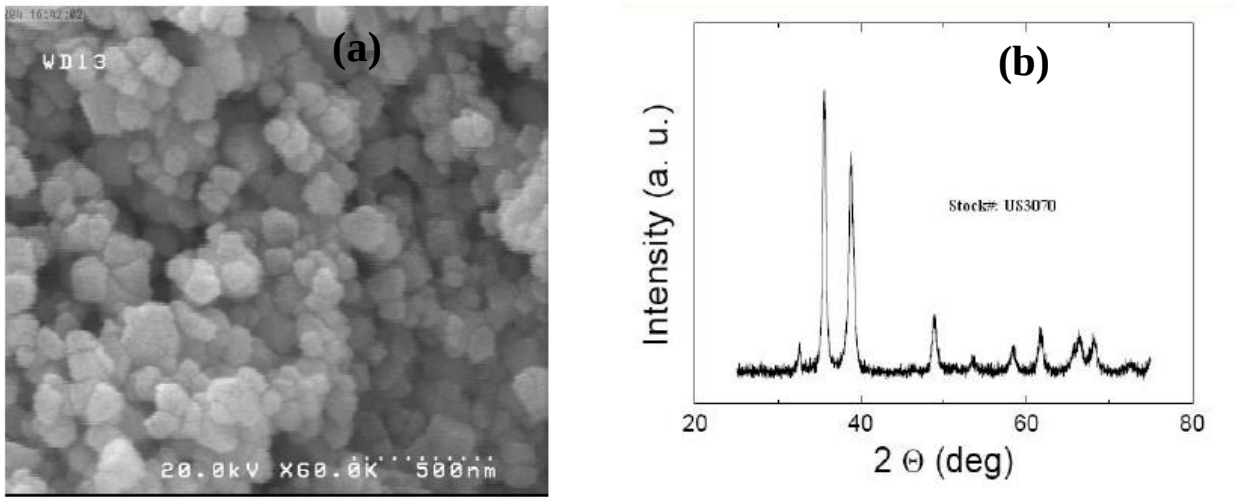

Figure 4 Analysis of the size and structural characteristics of copper oxide nanoparticles (**a)** TEM image of copper oxide nanoparticles (**b)** X-ray diffraction graph

2.2 Terminology in experimental design

Taguchi was the first to suggest that statistically planned experiments should be used in the product development stage to detect factors that affect variability of the output termed dispersion effects of the factors. He argued that by setting the factors with important dispersion effects at their optimal levels, the output can be made robust to changes in the operating and environmental conditions during production. Thus, the identification of dispersion effect is important to improve the quality of a process. In order to achieve a robust product/process one has to consider both location effect and dispersion effect. Taguchi has suggested a combined measure of both these effects. Suppose m is the mean effect and σ2 represent variance (dispersion effect). These two measures are combined into a single measure represented by m2/σ2. In terms of communications engineering terminology m2 may be termed as the power of the signal and σ2 may be termed as the power of noise and is called the Signal to Noise Ratio (S/N ratio or SNR). The data is transformed into S/N ratio and analyzed using ANOVA and then optimal levels for the factors is determined [28] . This leads to the development of the robust process or product. In Taguchi methods, the concept of optimization means determination of best levels for the control main factors that minimizes the effect of noise factors. The best levels of control main factors are those that maximize the signal to noise or S/N ratio. Based on the Taguchi method, effective main factors in experiments have been divided into two structural type: controllable (signal factors) and uncontrollable (disturbance or noise factors). In this case, signal-to-noise factors ratio analysis has used to determine the best execution of experiments or the best combination of levels for different main factors and achievement of the optimal response.

Based on the above description, actually in the Taguchi method has been suggested the use of Orthogonal Arrays or OAs for designing the experiments. On the other hand by this method the concept of linear graphs which simplifies the design of Orthogonal Arrays experiments has been also developed. These designs can be applied by engineers/scientists without acquiring advanced statistical knowledge. The main advantage of these designs lies in their simplicity, easy adaptability to more complex experiments involving number of factors with different numbers of levels. They provide the desired information with the least possible number of trials and yet yield reproducible results with adequate precision. These methods are usually employed to study main effects and applied in screening/pilot experiments. By experimental design to carry out sensitivity analysis, the Taguchi method with L16 orthogonal array and statistical analysis of variance (ANOVA) have been utilized. The response of the output

variable from the process or on the other words characteristic factors have measured at the end of the experiment, and the optimal conditions have determined based on the closeness to the response goals therefore, the responses have also classified and evaluated as follows [28]:

1. The Best Nominal Response: It has been used when the goal is to reach or to get close of a number that the design criterion.
2. The Best Bigger Response: When the upper limit of the response measured at the end of the experiment has been considered.
3. The Best Smaller Response: When the lower limit of the response measured at the end of the experiment has been considered.

In this research, the thermal conductivity and viscosity of nanofluids has been investigated. In this regard, the best response for the highest thermal conductivity and the lowest viscosity, respectively have been checked. Therefore, using Minitab software and Taguchi's method, based on the more thermal conductivity, better thermal performance and lower viscosity, better thermal performance, the research path pattern and the number of test steps have been determined. Variable levels of experiment, in order to determine the influence of the main factors have been considered and that In each of these experiments, the values of these main factors while till to complete the matrix of Taguchi variables have been different. Then, according to this point, the higher thermal conductivity and the lower viscosity, it has been the best. Main factors and the number of experiments in the role of each operational factors have been determined.

Table 4 Main factors and levels in the thermal conductivity experiments

Main factors	Level 1	Level 2	Level 3	Level 4
Volume Fraction (%)	0.1	0.2	0.3	0.4
Temperature (˚C)	25	30	35	40

Table 5 Experimental design by using the orthogonal arrangement L16 of Taguchi method for the thermal conductivity

Experiment No.	Levels of Temperature	Levels of Volume Fraction
1	1	1
2	1	2
3	1	3
4	1	4
5	2	1
6	2	2
7	2	3
8	2	4
9	3	1
10	3	2
11	3	3
12	3	4
13	4	1
14	4	2
15	4	3
16	4	4

Table 6 Main factors and levels in the viscosity experiments

Main factors	Level 1	Level 2	Level 3	Level 4
Volume Fraction (%)	0.1	0.2	0.3	0.4
Temperature (°C)	25.3	27.6	30.7	40

Table 7 Experimental design by using the orthogonal arrangement L16 of Taguchi method for the viscosity

Experiment No.	Levels of Volume Fraction	Levels of Temperature
1	1	1
2	1	2
3	1	3
4	1	4
5	2	1
6	2	2
7	2	3
8	2	4
9	3	1
10	3	2
11	3	3
12	3	4
13	4	1
14	4	2
15	4	3
16	4	4

After the experiments, by analyzing the signal-to-noise ratio, or SNR the role of each variables can be correctly determined. In general, the higher the SNR value, the closer to the target have been done. Based on this, according to Table (4) and Table (6), two main factors in the four levels have been considered. Then, by using the Taguchi method and the Minitab software, in order to the manner and the structural method of experiments have been completely determined. According to the relevant main factors and levels in Table (4) and (6), an orthogonal arrangement with the L16 array of Taguchi method to design the experiments have been applied. In this way, the results of these arrangements have presented in Table (5) and Table (7).

The Main Experiments: In this way, according to the experimental design, *thermal conductivity and dynamic viscosity* of nanofluids have been measured in four different volume concentrations (0.1, 0.2, 0.3, and 0.4%) and at different temperatures by using related measuring equipment, and that the results have been plotted as the some certain graphs.

2.3 The thermal conductivity

The first experiment: This experiment by nanofluid with volume concentration of 0.1% at different temperatures has performed as it's presented in Table (8). Proposed quadratic and cubic models by the experimental data of thermal conductivity with respect to temperature at 0.1 vol.% concentration have been presented in Figure (5) and Figure (6) respectively.

Table 8 The thermal conductivity values of nanofluid with the concentration of 0.1 vol% at different temperatures

T (˚C)	T (K)	k_f(w/m.K)	k_{nf} (w/m.K)	k_{nf}/k_f
25	298.15	0.5313	0.5513	1.037644
27.5	300.65	0.5384	0.5715	1.061478
30	303.15	0.5412	0.5801	1.071877
32.5	305.65	0.5521	0.5921	1.072451
35	308.15	0.5624	0.6101	1.084815
37.5	310.65	0.5728	0.6265	1.09375
40	313.5	0.5866	0.6459	1.107228

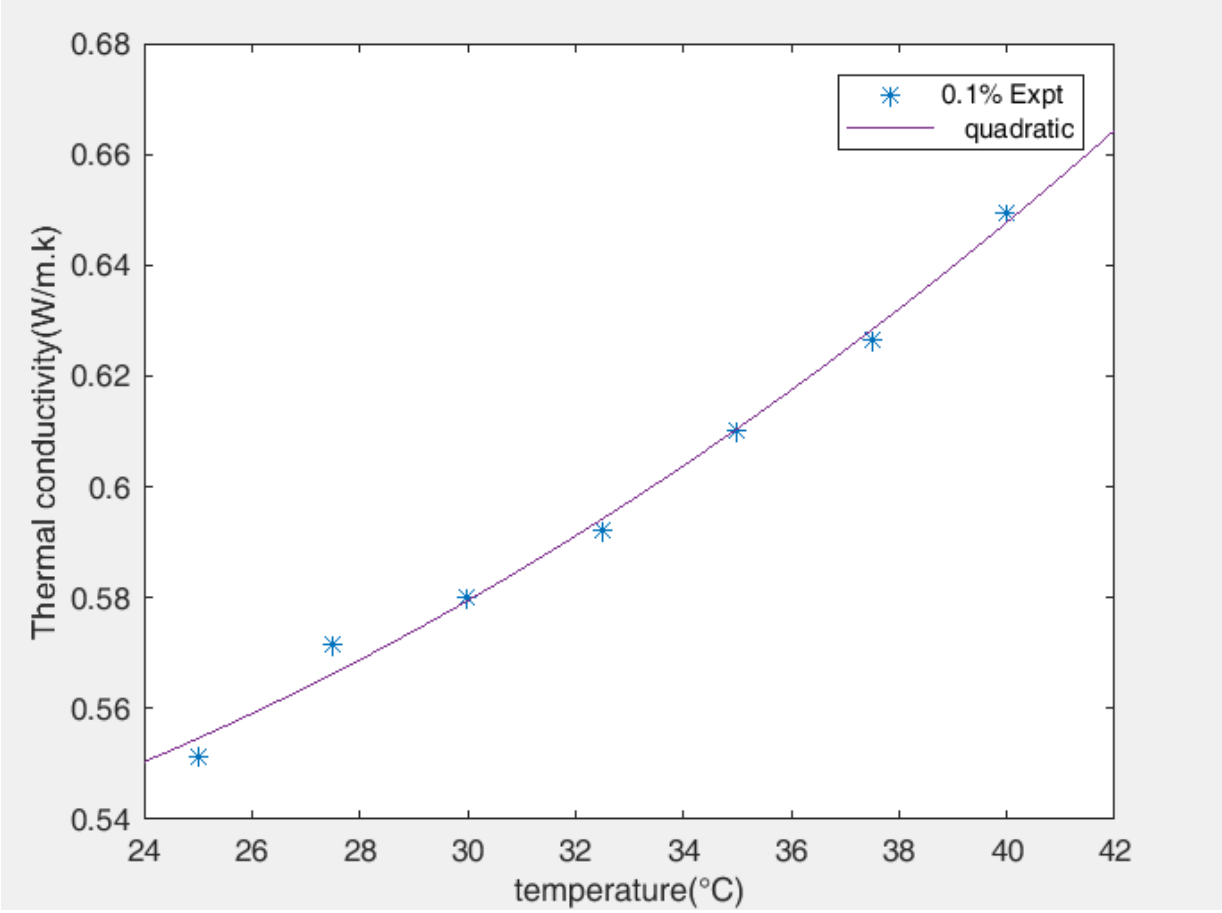

Figure 5 Proposed quadratic model by the experimental data of thermal conductivity with respect to temperature in 0.1 vol.% concentration

$$k = 0.00012\,T^2 - 0.0018\,T + 0.52 \quad (1)$$

$$k = 2.3 \times 10^{-5}T^3 - 0.0022T^2 + 0.071T - 0.25 \quad (2)$$

The second experiment: This experiment by nanofluid with volume concentration of 0.2 vol.% at different temperatures has performed as it's presented in Table (9). Proposed linear model by the experimental data of thermal conductivity with respect to temperature at 0.2 vol.% concentration have been presented in Figure (7).

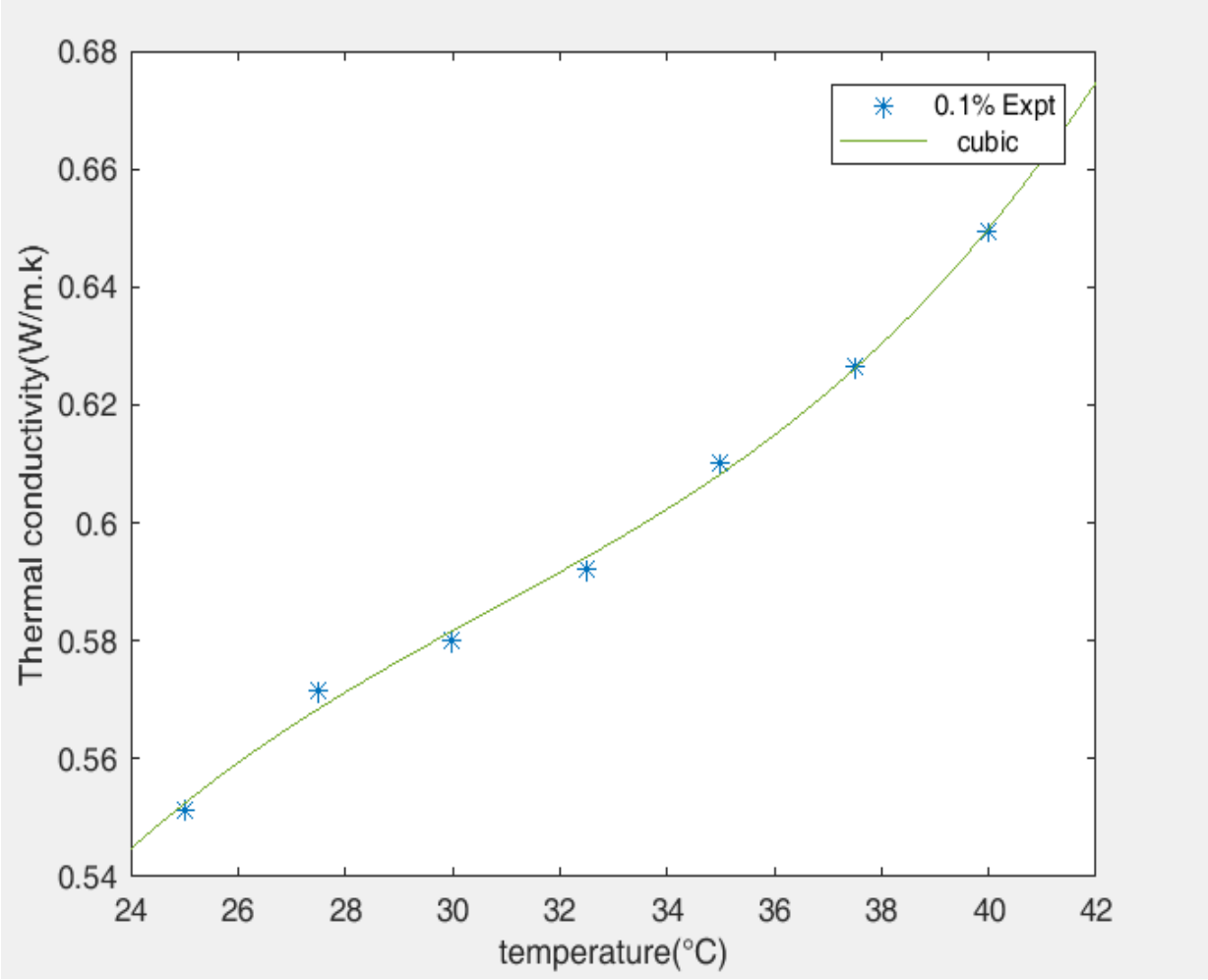

Figure 6 Proposed cubic model by the experimental data of thermal conductivity with respect to temperature in 0.1 vol.% concentration

Table 9 The thermal conductivity values of nanofluid with the concentration of 0.2 vol% at different temperatures

T (˚C)	T (K)	k_f(w/m.K)	k_{nf} (w/m.K)	k_{nf}/k_f
25	298.15	0.5313	0.5962	1.122153
27.5	300.65	0.5384	0.6215	1.154346
30	303.15	0.5412	0.6385	1.179786
32.5	305.65	0.5521	0.6615	1.198153
35	308.15	0.5624	0.6845	1.217105
37.5	310.65	0.5728	0.7044	1.229749
40	313.5	0.5866	0.725	1.235936

$$k = 0.0085\ T + 0.38 \quad (3)$$

The third experiment: This experiment by nanofluid with volume concentration of 0.3 vol.% at different temperatures has performed as it's presented in Table (10). Proposed quadratic model by the experimental data of thermal conductivity with respect to temperature at 0.3 vol.% concentration have been presented in Figure (8).

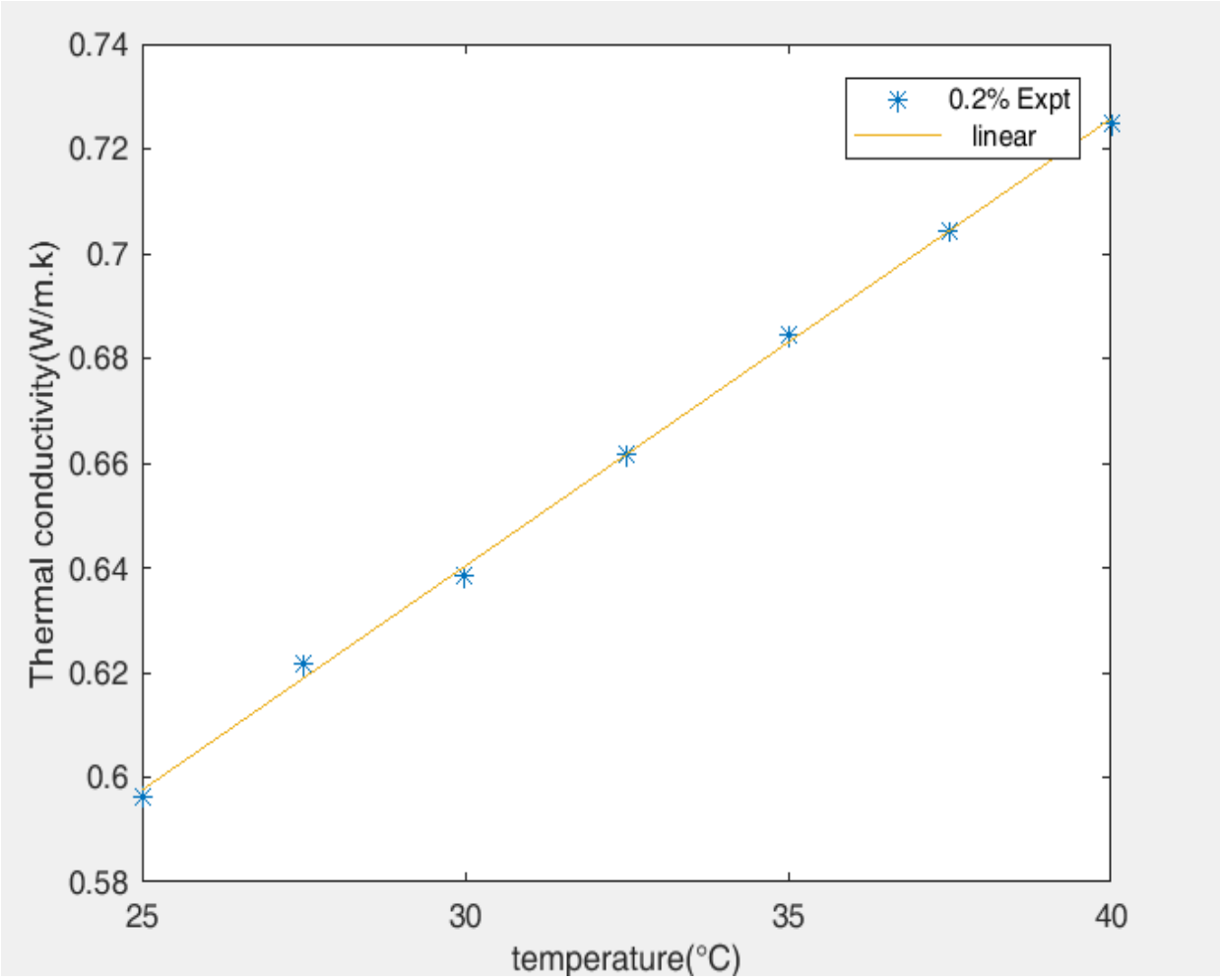

Figure 7 Proposed linear model by the experimental data of thermal conductivity with respect to temperature in 0.2 vol.% concentration

Table 10 The thermal conductivity values of nanofluid with the concentration of 0.3 vol% at different temperatures

T (°C)	T (K)	k_f(w/m.K)	k_{nf} (w/m.K)	k_{nf}/k_f
25	298.15	0.5313	0.6342	1.193676
27.5	300.65	0.5384	0.6485	1.204495
30	303.15	0.5412	0.6701	1.238174
32.5	305.65	0.5521	0.6886	1.247238
35	308.15	0.5624	0.7065	1.256223
37.5	310.65	0.5728	0.7325	1.278806
40	313.5	0.5866	0.7584	1.292874

$$k = 0.00015T^2 - 0.0015T + 0.58 \quad (4)$$

The fourth experimen: This experiment by nanofluid with volume concentration of 0.4 vol.% at different temperatures has performed as it's presented in Table (11). Proposed quadratic and cubic models by the experimental data of thermal conductivity with respect to temperature at 0.4 vol. % concentration have been presented in Figure (9) and Figure (10) respectively.

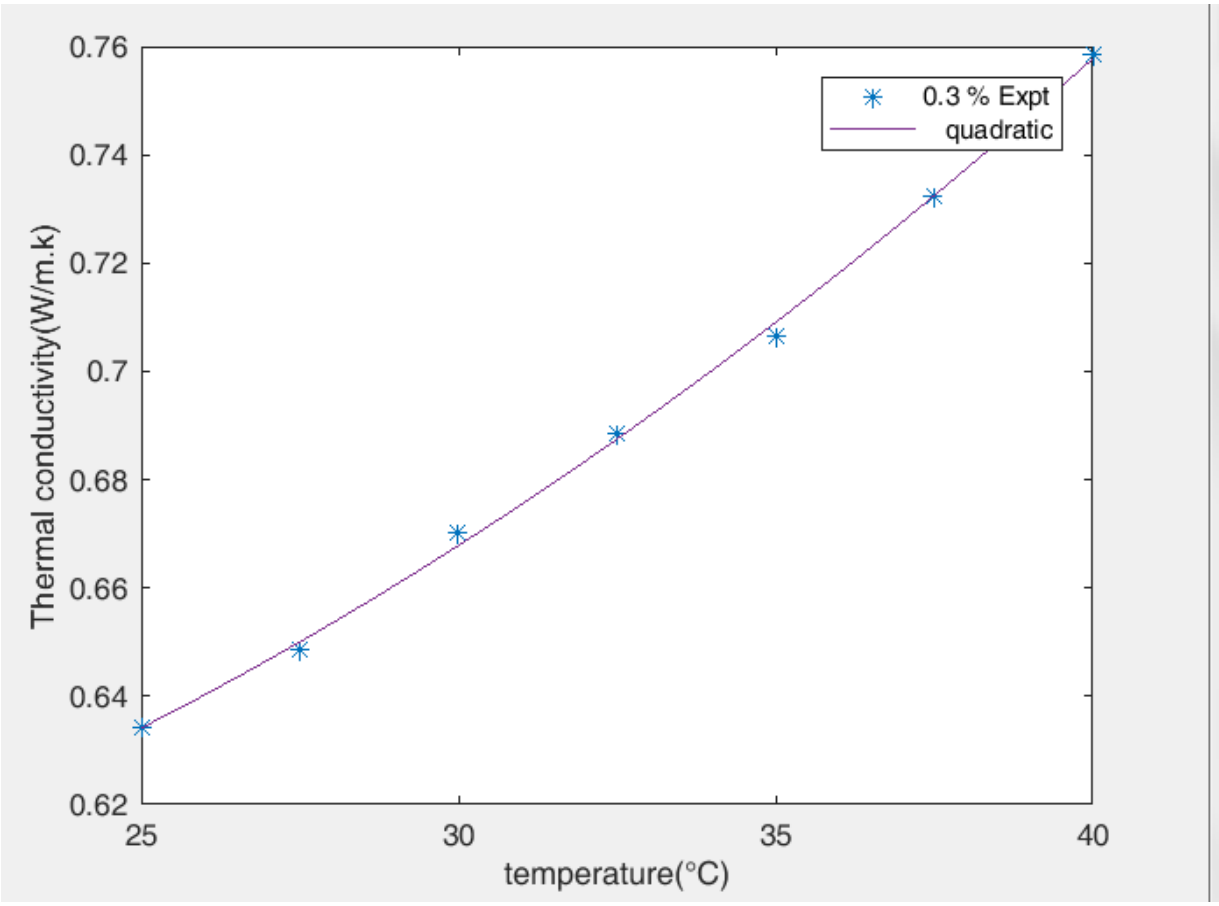

Figure 8 Proposed quadratic model by the experimental data of thermal conductivity with respect to temperature in 0.3 vol.% concentration

Table 11 The thermal conductivity values of nanofluid with the concentration of 0.4vol% at different temperatures

T (˚C)	T (K)	k_f(w/m.K)	k_{nf} (w/m.K)	k_{nf}/k_f
25	298.15	0.5313	0.6523	1.227743
27.5	300.65	0.5384	0.6626	1.230684
30	303.15	0.5412	0.6783	1.253326
32.5	305.65	0.5521	0.6976	1.263539
35	308.15	0.5624	0.7286	1.295519
37.5	310.65	0.5728	0.7573	1.322102
40	313.5	0.5866	0.7825	1.333958

$$k = 0.00031T^2 - 0.011T + 0.74 \quad (5)$$

$$k = -2.6 \times 10^{-5}T^3 + 0.0029T^2 - 0.093T + 1.6 \quad (6)$$

The fifth experiment: This experiment has been done for nanofluid at 25°C in different concentrations as it's presented in Table (12). Proposed quadratic model by the experimental data of thermal conductivity ratio by increasing the concentration at 25°C has been presented in Figure (11).

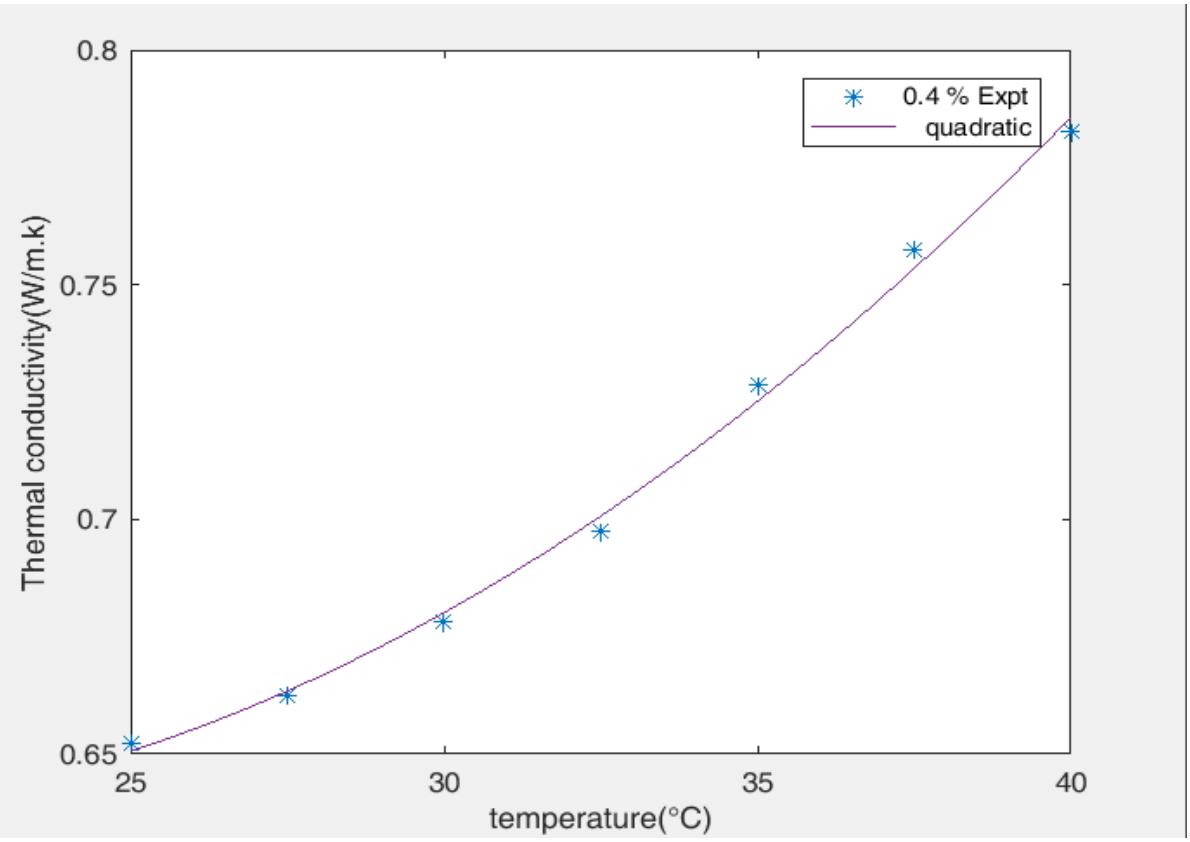

Figure 9 Proposed quadratic model by the experimental data of thermal conductivity with respect to temperature in 0.4 vol.% concentration

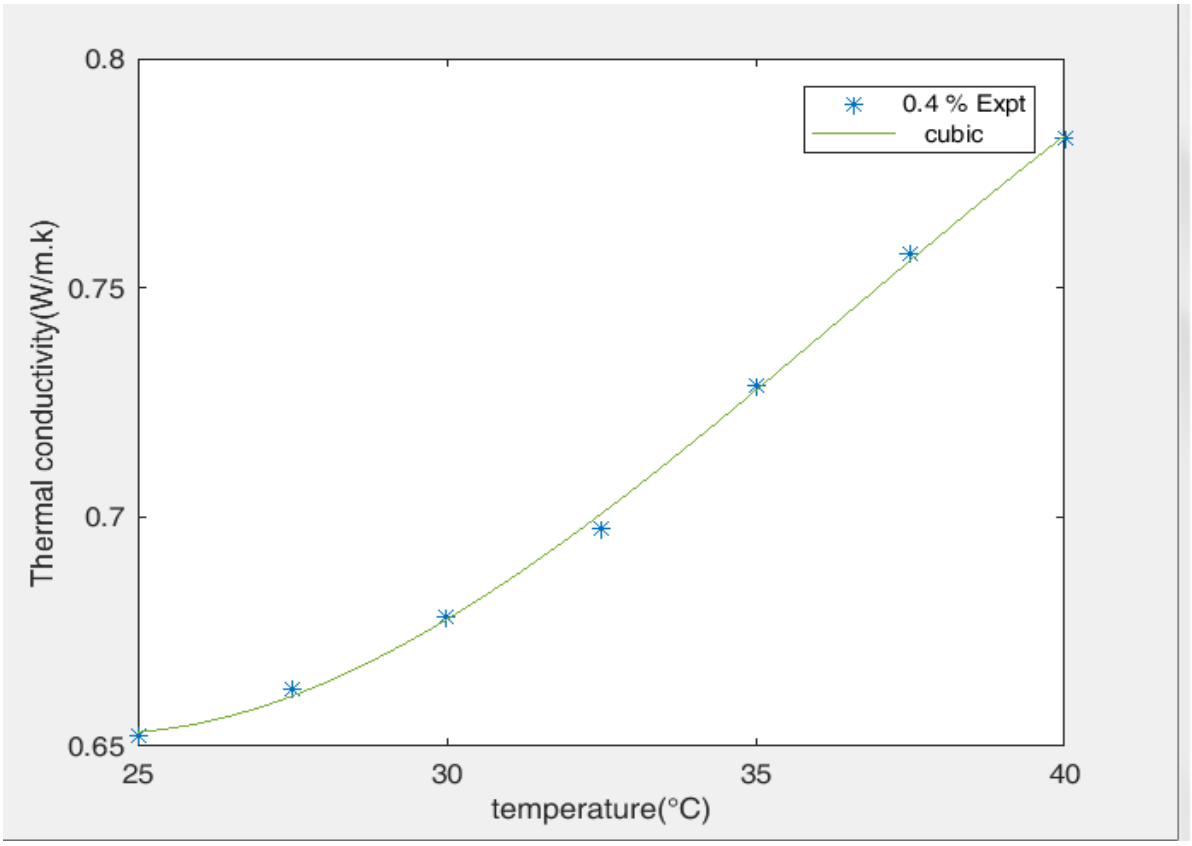

Figure 10 Proposed cubic model by the experimental data of thermal conductivity with respect to temperature in 0.4 vol.% concentration.

Table 12 The thermal conductivity ratio of nanofluid by increasing the concentration at 25°C

φ (vol. %)	$\frac{k_{nf}}{k_f}$
0.1	1.037644
0.2	1.122153
0.3	1.193676
0.4	1.227743

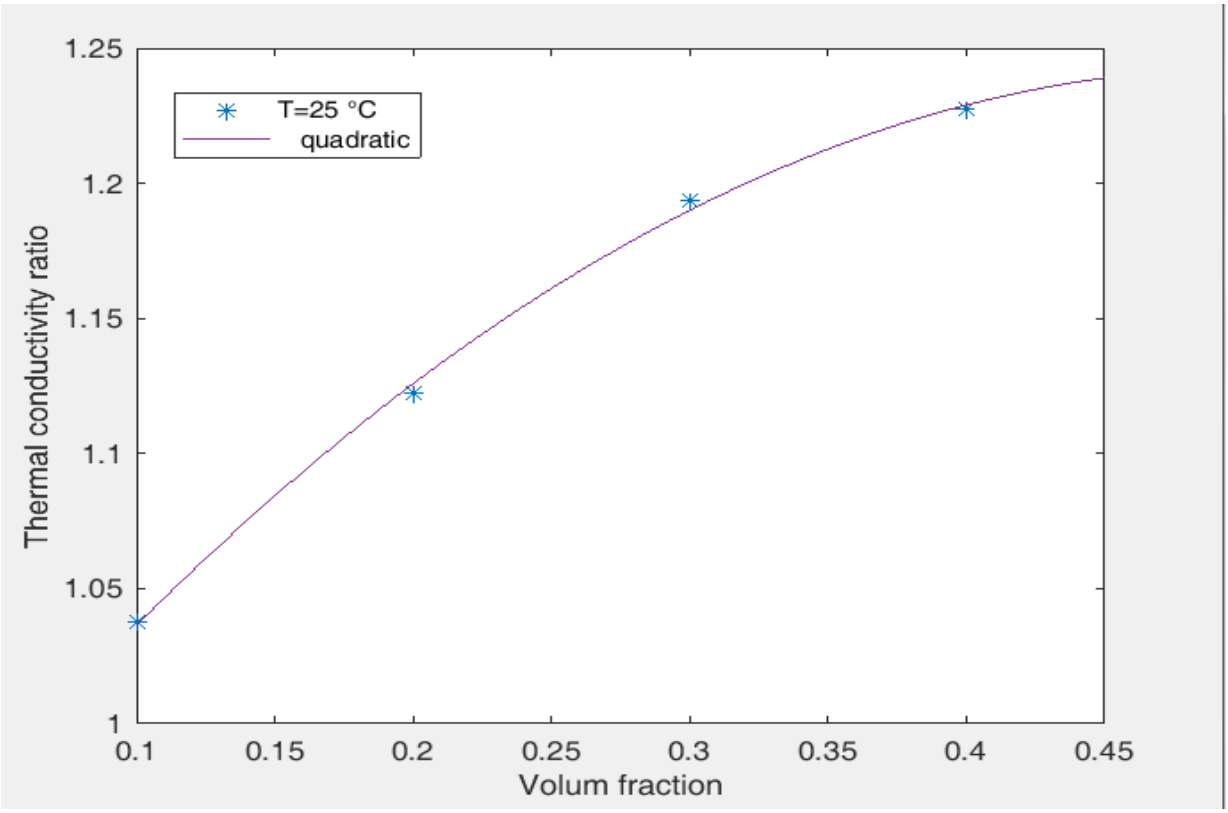

Figure 11 Proposed quadratic model by the experimental data of thermal conductivity ratio by increasing the concentration at 25°C

$$\frac{k_{nf}}{k_f} = -1.3\varphi^2 + 1.3\varphi + 0.92 \quad (7)$$

The sixth experiment: This experiment has been done for nanofluid at 30°C in different concentrations as it's presented in Table (13). Proposed quadratic model by the experimental data of thermal conductivity ratio by increasing the concentration at 30°C has been presented in Figure (12).

$$\frac{k_{nf}}{k_f} = -2.3\varphi^2 + 1.8\varphi + 0.92 \quad (8)$$

The seventh experiment: This experiment has been done for nanofluid at 35°C in different concentrations as it's presented in Table (14). Proposed quadratic model by the experimental data of thermal conductivity ratio by increasing the concentration at 35°C has been presented in Figure (13).

Table 13 The thermal conductivity ratio of nanofluid by increasing the concentration at 30°C

φ(vol. %)	$\frac{k_{nf}}{k_f}$
0.1	1.071877
0.2	1.179786
0.3	1.238174
0.4	1.253326

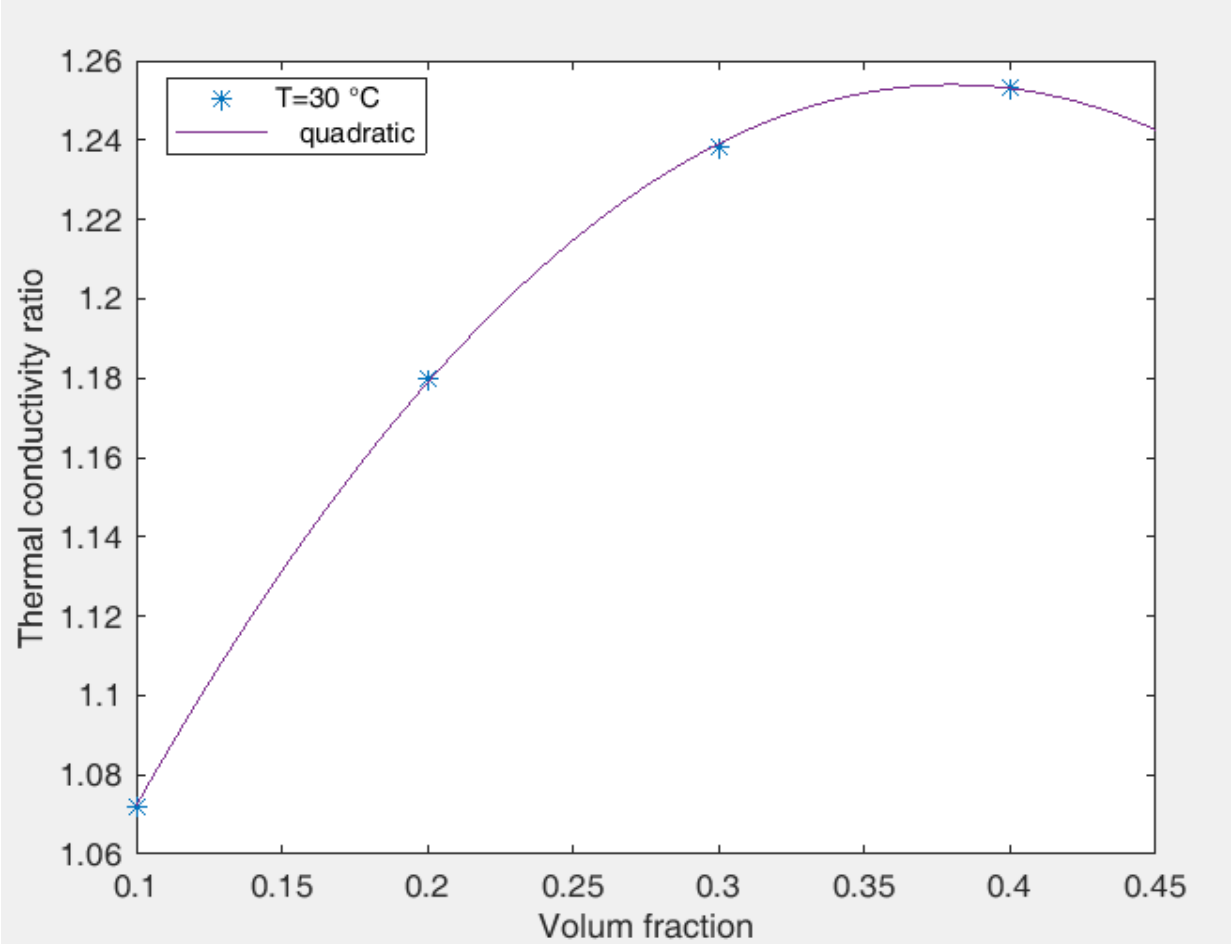

Figure 12 Proposed quadratic model by the experimental data of thermal conductivity ratio by increasing the concentration at 30°C

Table 14 The thermal conductivity ratio of nanofluid by increasing the concentration at 35°C

φ (vol. %)	$\frac{k_{nf}}{k_f}$
0.1	1.071877
0.2	1.179786
0.3	1.238174
0.4	1.253326

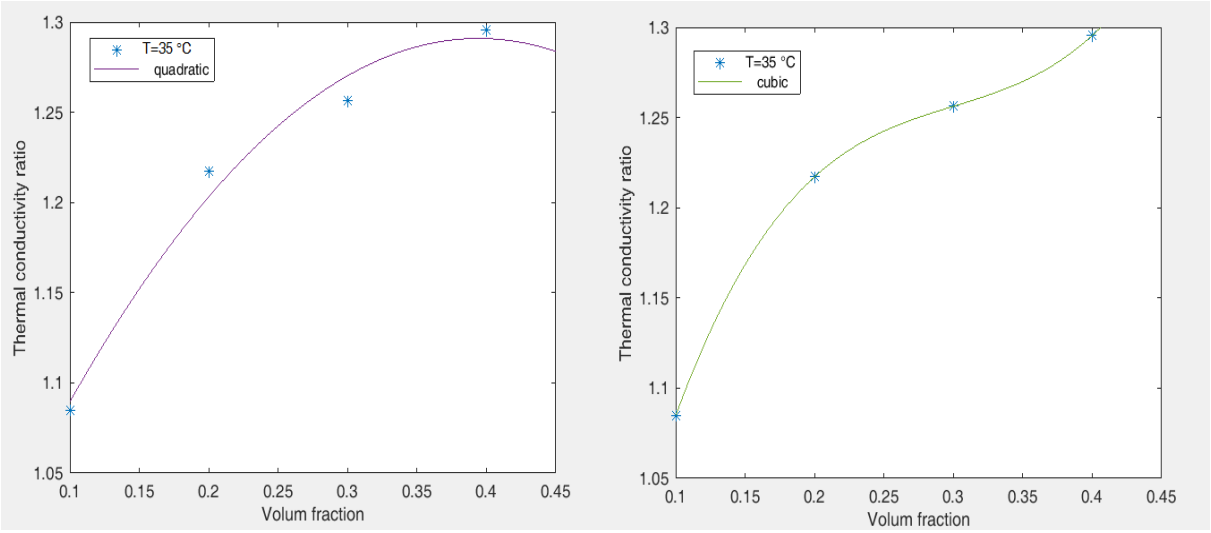

Figure 13 Proposed quadratic and cubic models by the experimental data of thermal conductivity ratio by increasing the concentration at 35°C

Table 15 The thermal conductivity ratio of nanofluid by increasing the concentration at 40°C

φ (vol. %)	$\frac{k_{nf}}{k_f}$
0.1	1.107228
0.2	1.235936
0.3	1.292874
0.4	1.333958

$$\frac{k_{nf}}{k_f} = -2.3\varphi^2 + 1.8\varphi + 0.93 \quad (9)$$

$$\frac{k_{nf}}{k_f} = 16\varphi^3 - 14\varphi^2 + 4.4\varphi + 0.77 \quad (10)$$

The eighth experiment: This experiment has been done for nanofluid at 40°C in different concentrations as it's presented in Table (15). Proposed quadratic model by the experimental data of thermal conductivity ratio by increasing the concentration at 40°C has been presented in Figure (14).

$$\frac{k_{nf}}{k_f} = -2.2\varphi^2 + 1.8\varphi + 0.95 \quad (11)$$

2.4 The dynamic viscosity

The first experiment: This experiment by nanofluid with volume concentration of 0.1% at different temperatures has performed as it's presented in Table (16). Proposed linear and quadratic models by the experimental data of dynamic viscosity with respect to temperature at 0.1 vol.% concentration have been presented in Figure (15) and Figure (16) respectively.

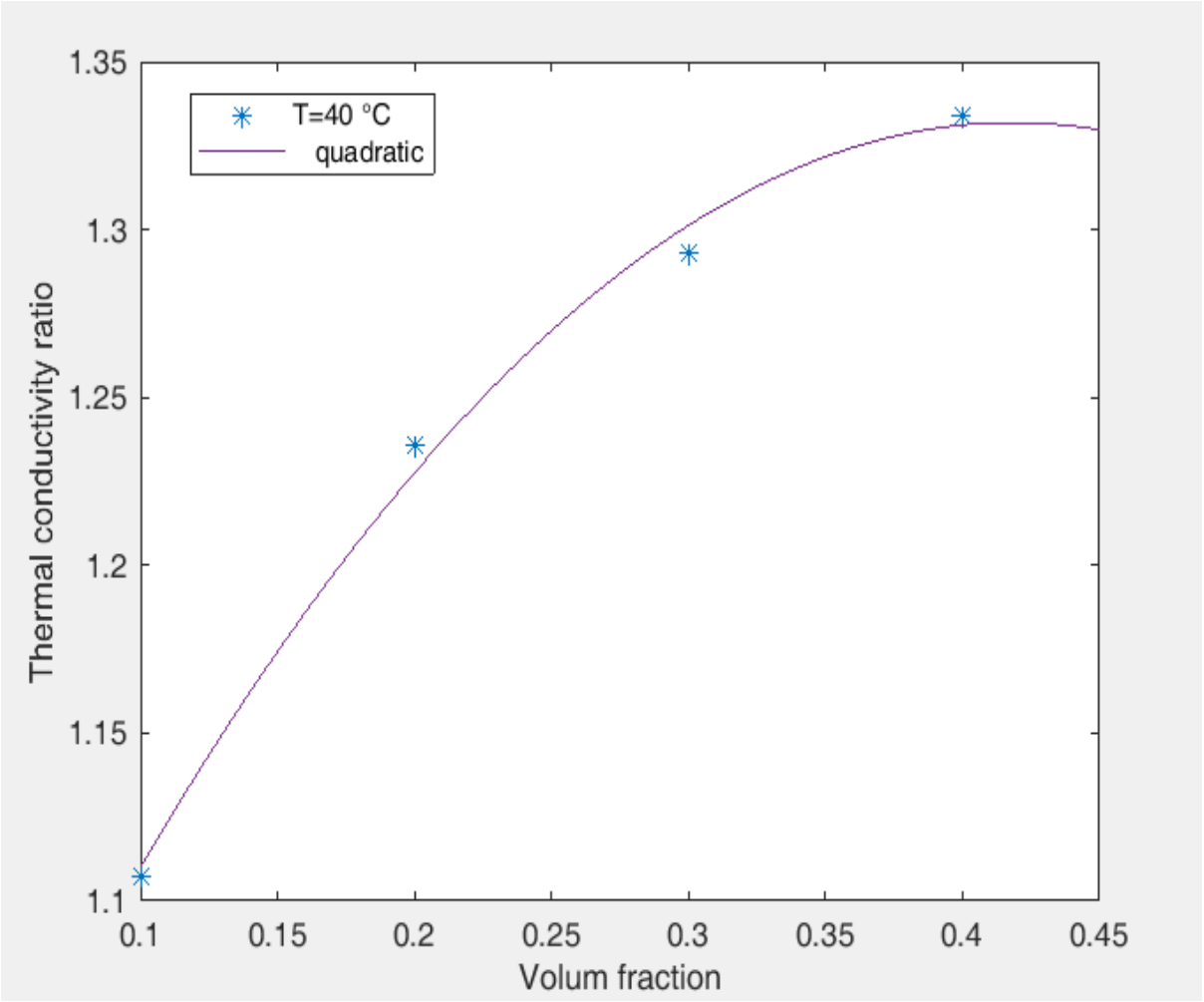

Figure 14 Proposed quadratic model by the experimental data of thermal conductivity ratio by increasing the concentration at 40°C

$$\mu_{nf} = -1.6 \times 10^{-5}T + 0.0012 \tag{12}$$

$$\mu_{nf} = -2.8 \times 10^{-7}T^2 + 9.3 \times 10^{-7}T + 0.001 \tag{13}$$

The second experiment: This experiment by nanofluid with volume concentration of 0.2% at different temperatures has performed as it's presented in Table (17). Proposed linear and quadratic models by the experimental data of dynamic viscosity with respect to temperature at 0.2 vol.% concentration have been presented in Figure (17) and Figure (18) respectively.

$$\mu_{nf} = -1.5 \times 10^{-5}T + 0.0012 \tag{14}$$

$$\mu_{nf} = -3.5 \times 10^{-7}T^2 + 5.3 \times 10^{-6}T + 0.00095 \tag{15}$$

The third experiment: This experiment by nanofluid with volume concentration of 0.3% at different temperatures has performed as it's presented in Table (18). Proposed linear and quadratic models by the experimental data of dynamic viscosity with respect to temperature at 0.3 vol.% concentration have been presented in Figure (19) and Figure (20) respectively.

Table 16 The Dynamic Viscosity values of nanofluid with the concentration of 0.1 vol% at different temperatures

T (°C)	T (K)	μ_f (Pa.s)	μ_{nf} (Pa.s)
25.3	298.45	0.000825	0.000851
25.5	298.65	0.000823	0.000848
25.8	298.95	0.00082	0.000845
26.1	299.25	0.000821	0.000846
26.6	299.75	0.000809	0.000834
27	300.15	0.000809	0.000834
27.6	300.75	0.000794	0.000819
28.1	301.25	0.00079	0.000814
28.6	301.75	0.000783	0.000807
29.2	302.35	0.000771	0.000795
29.7	302.85	0.000769	0.000793
30.2	303.35	0.000753	0.000776
30.7	303.85	0.000751	0.000774
31.3	304.45	0.000737	0.00076
31.8	304.95	0.00073	0.000753
32.3	305.45	0.000725	0.000747
32.8	305.95	0.000711	0.000733
33.3	306.45	0.000711	0.000733

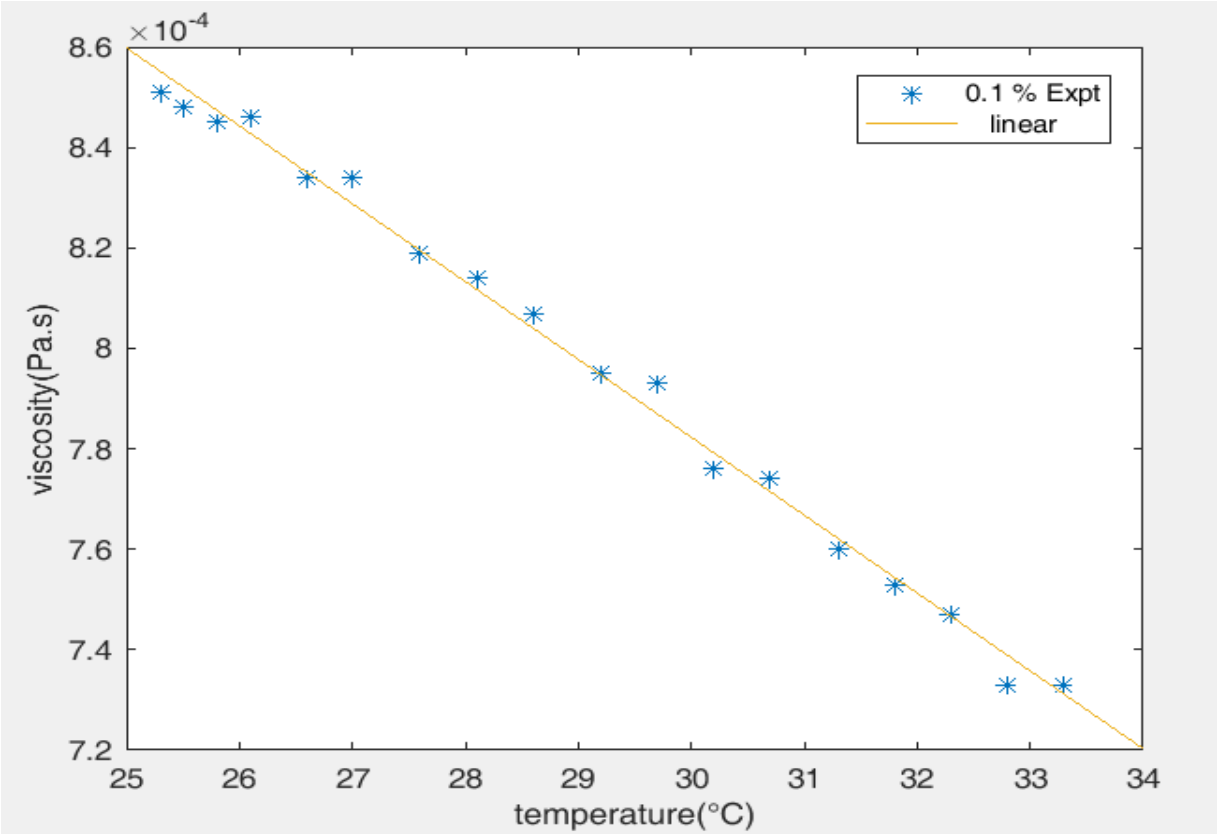

Figure 15 Proposed linear model by the experimental data of dynamic viscosity with respect to temperature in 0.1 vol.% concentration

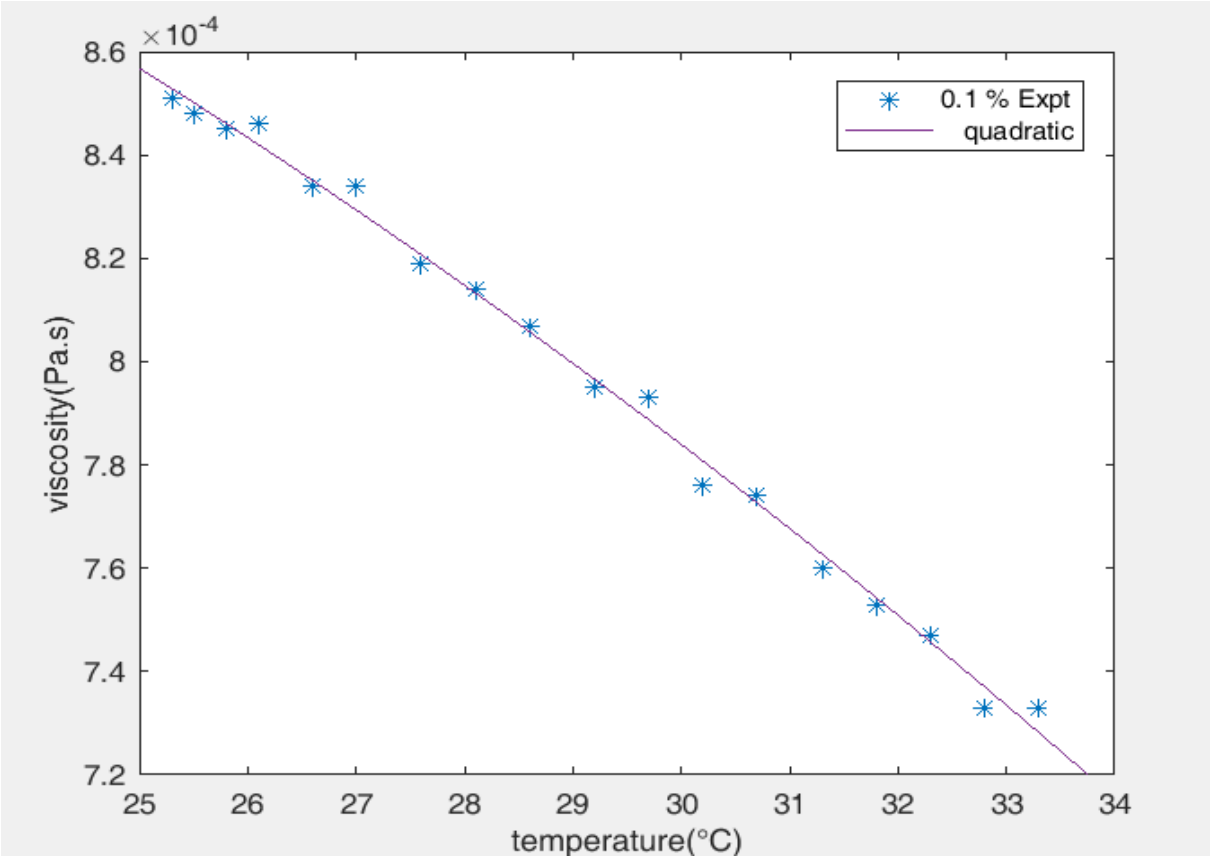

Figure 16 Proposed quadratic model by the experimental data of dynamic viscosity with respect to temperature in 0.1 vol.% concentration

Table 17 The dynamic viscosity values of nanofluid with the concentration of 0.2 vol% at different temperatures

T (°C)	T (K)	μ_f (Pa.s)	μ_{nf} (Pa.s)
25.3	298.45	0.000825	0.000851
25.5	298.65	0.000823	0.00085
25.8	298.95	0.00082	0.000848
26.1	299.25	0.000821	0.00085
26.6	299.75	0.000809	0.000837
27	300.15	0.000809	0.000838
27.6	300.75	0.000794	0.000823
28.1	301.25	0.00079	0.000819
28.6	301.75	0.000783	0.000811
29.2	302.35	0.000771	0.0008
29.7	302.85	0.000769	0.000797
30.2	303.35	0.000753	0.000779
30.7	303.85	0.000751	0.000778
31.3	304.45	0.000737	0.000763
31.8	304.95	0.00073	0.000758
32.3	305.45	0.000725	0.000751
32.8	305.95	0.000711	0.000738
33.3	306.45	0.000711	0.000738

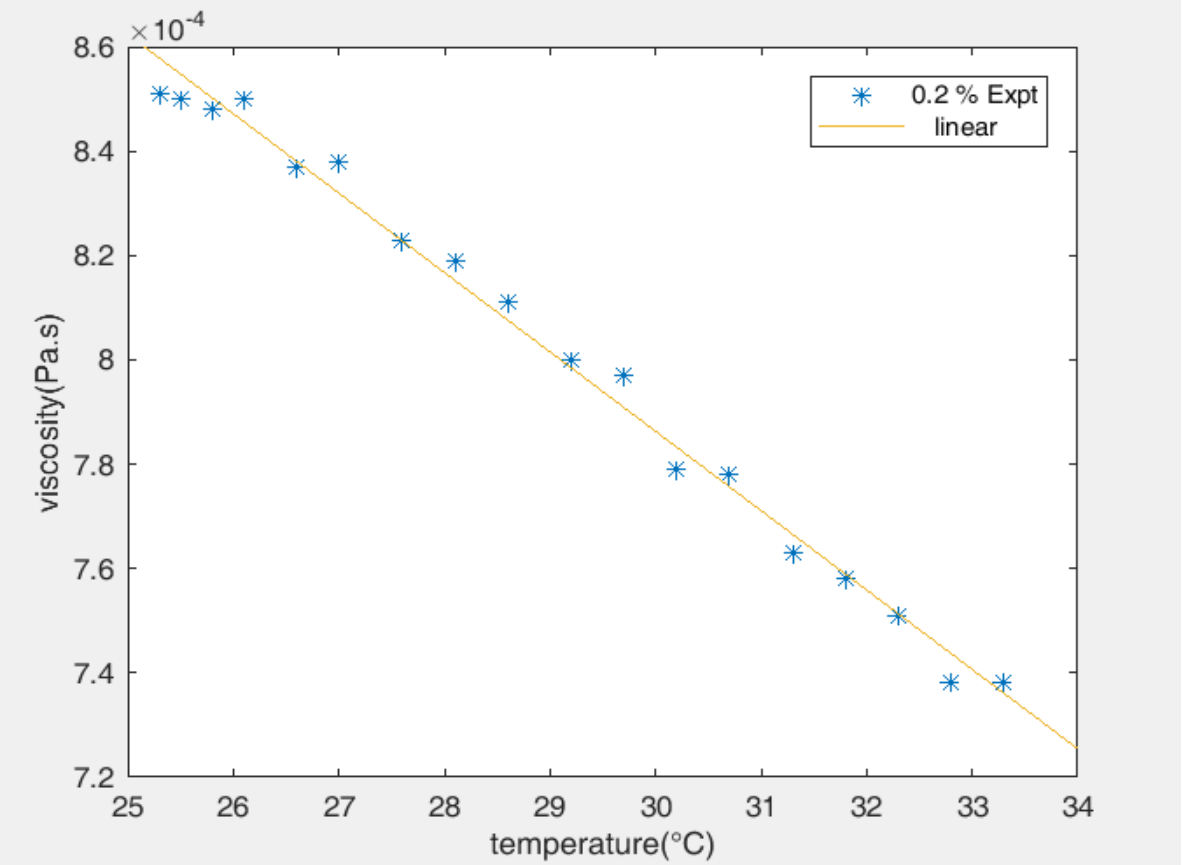

Figure 17 Proposed linear model by the experimental data of dynamic viscosity with respect to temperature in 0.2 vol.% concentration

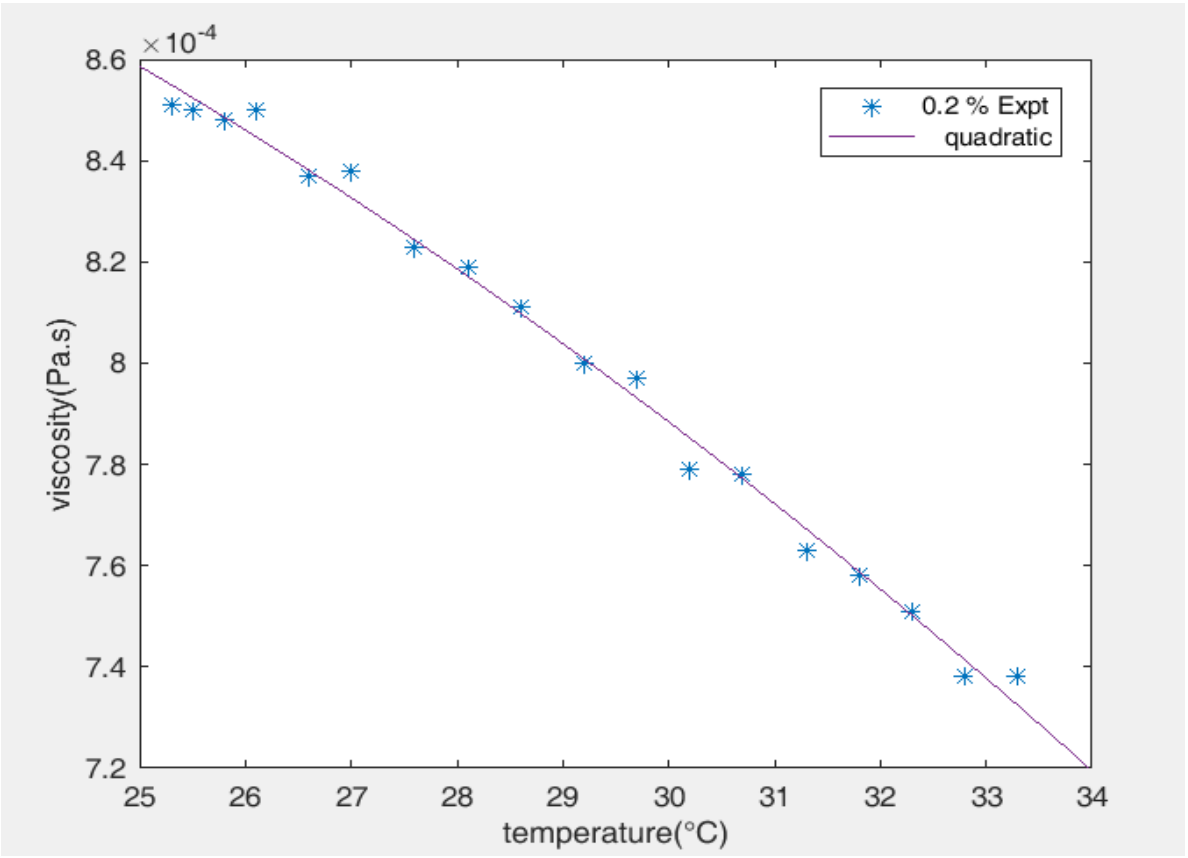

Figure 18 Proposed quadratic model by the experimental data of dynamic viscosity with respect to temperature in 0.2 vol.% concentration

Table 18 The dynamic viscosity values of nanofluid with the concentration of 0.3 vol% at different temperatures

T (°C)	T (K)	μ_f (Pa.s)	μ_{nf} (Pa.s)
25.3	298.45	0.000825	0.000865
25.5	298.65	0.000823	0.000858
25.8	298.95	0.00082	0.000853
26.1	299.25	0.000821	0.000853
26.6	299.75	0.000809	0.000839
27	300.15	0.000809	0.000841
27.6	300.75	0.000794	0.000824
28.1	301.25	0.00079	0.000822
28.6	301.75	0.000783	0.000814
29.2	302.35	0.000771	0.000802
29.7	302.85	0.000769	0.000799
30.2	303.35	0.000753	0.000781
30.7	303.85	0.000751	0.000783
31.3	304.45	0.000737	0.000765
31.8	304.95	0.00073	0.00076
32.3	305.45	0.000725	0.000754
32.8	305.95	0.000711	0.000741
33.3	306.45	0.000711	0.000741

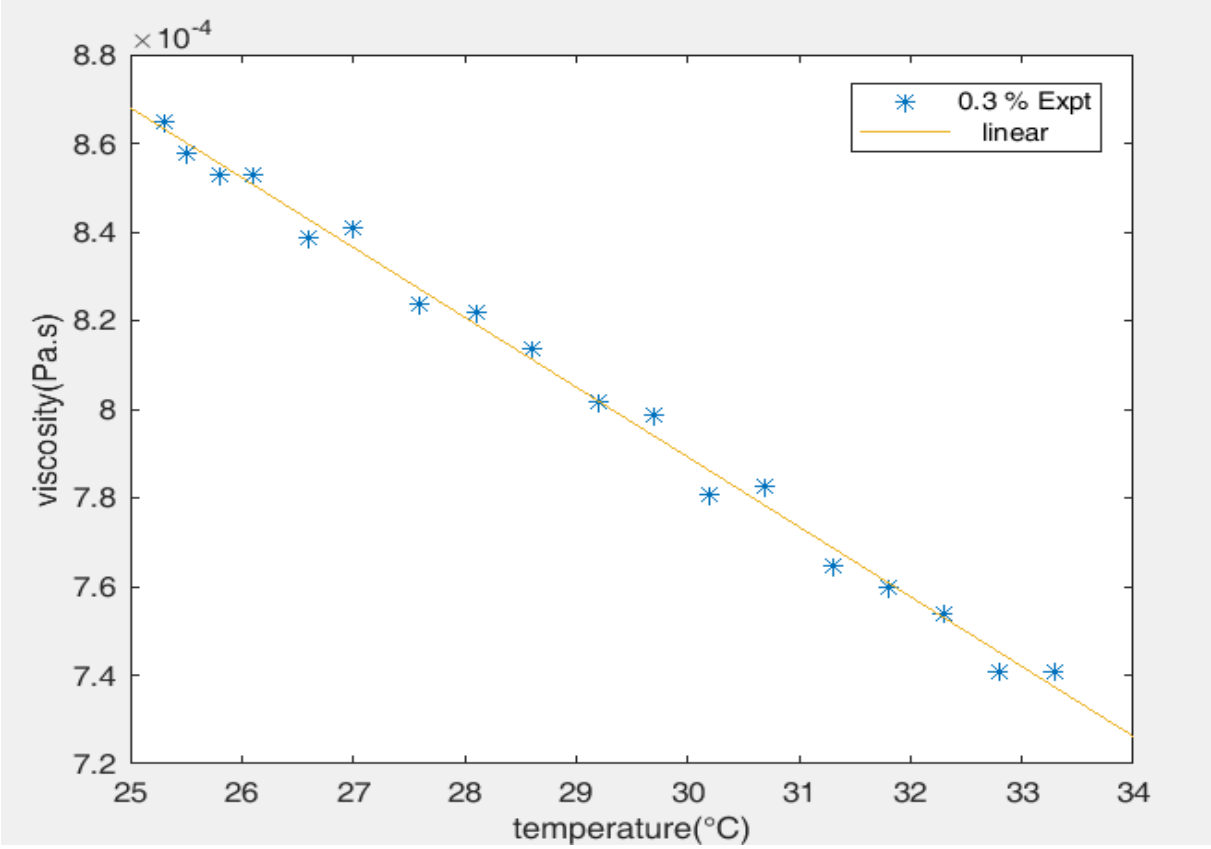

Figure 19 Proposed linear model by the experimental data of dynamic viscosity with respect to temperature in 0.3 vol.% concentration

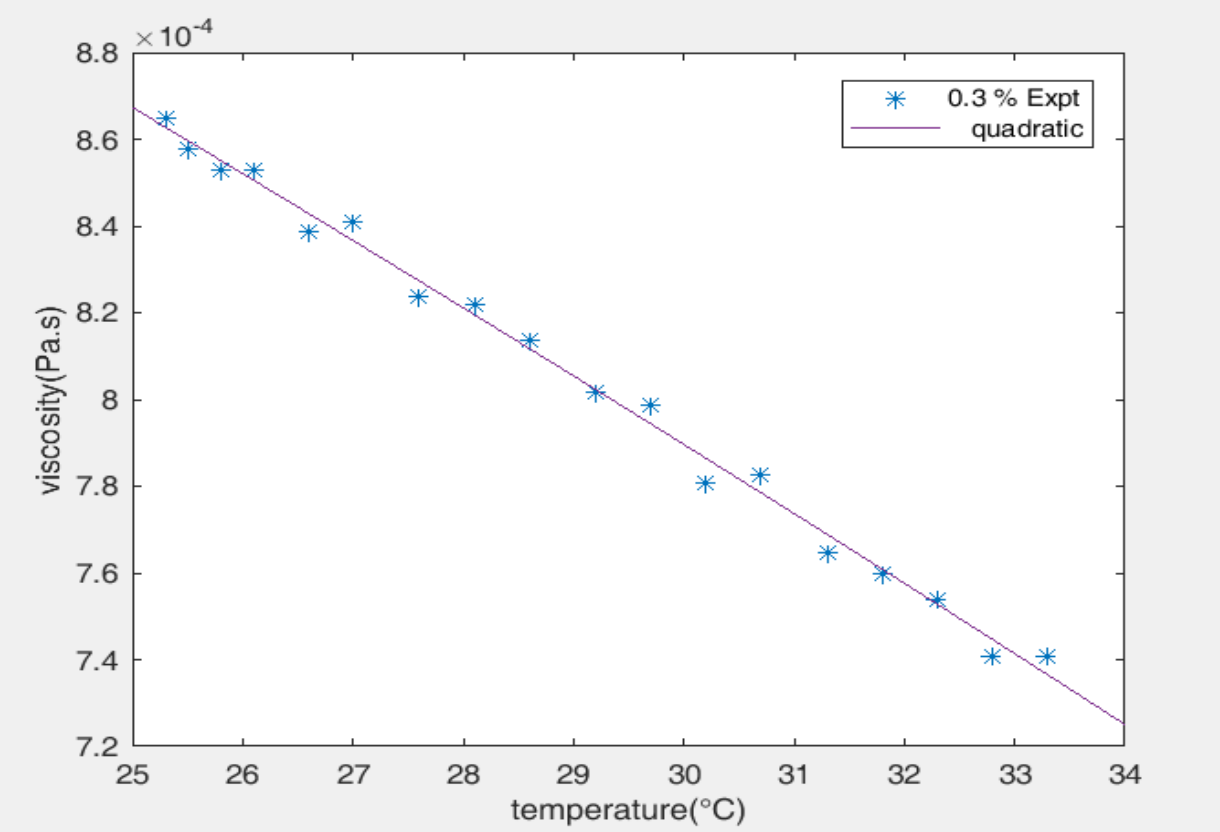

Figure 20 Proposed quadratic model by the experimental data of dynamic viscosity with respect to temperature in 0.3 vol.% concentration

Table 19 The dynamic viscosity values of nanofluid with the concentration of 0.4 vol% at different temperatures

T (°C)	T (K)	μ_f (Pa.s)	μ_{nf} (Pa.s)
25.3	298.45	0.000825	0.000868
25.5	298.65	0.000823	0.000866
25.8	298.95	0.00082	0.000863
26.1	299.25	0.000821	0.000866
26.6	299.75	0.000809	0.000851
27	300.15	0.000809	0.000853
27.6	300.75	0.000794	0.000836
28.1	301.25	0.00079	0.000835
28.6	301.75	0.000783	0.000826
29.2	302.35	0.000771	0.000813
29.7	302.85	0.000769	0.000812
30.2	303.35	0.000753	0.000794
30.7	303.85	0.000751	0.000793
31.3	304.45	0.000737	0.000776
31.8	304.95	0.00073	0.000772
32.3	305.45	0.000725	0.000764
32.8	305.95	0.000711	0.000752
33.3	306.45	0.000711	0.000752

$$\mu_{nf} = -1.6 \times 10^{-5}T + 0.0013 \quad (16)$$

$$\mu_{nf} = -6.7 \times 10^{-8}T^2 - 1.2 \times 10^{-5}T + 0.0012 \quad (17)$$

The fourth Experiment: This experiment by nanofluid with volume concentration of 0.4% at different temperatures has performed as it's presented in Table (19). Proposed linear and quadratic models by the experimental data of dynamic viscosity with respect to temperature at 0.4 vol.% concentration have been presented in Figure (21) and Figure (22) respectively.

$$\mu_{nf} = -1.5 \times 10^{-5}T + 0.0013 \quad (18)$$

$$\mu_{nf} = -3.1 \times 10^{-7}T^2 + 2.6 \times 10^{-6}T + 0.001 \quad (19)$$

The fifth experiment: This experiment has been done for nanofluid at 25.3°C in different concentrations as it's presented in Table (20). Proposed quadratic model by the experimental data of dynamic viscosity by increasing the concentration at 25.3°C has been presented in Figure (23).

$$\frac{\mu_{nf}}{\mu_f} = -5.1\varphi^3 + 3.9\varphi^2 - 0.81\varphi + 1.1 \quad (20)$$

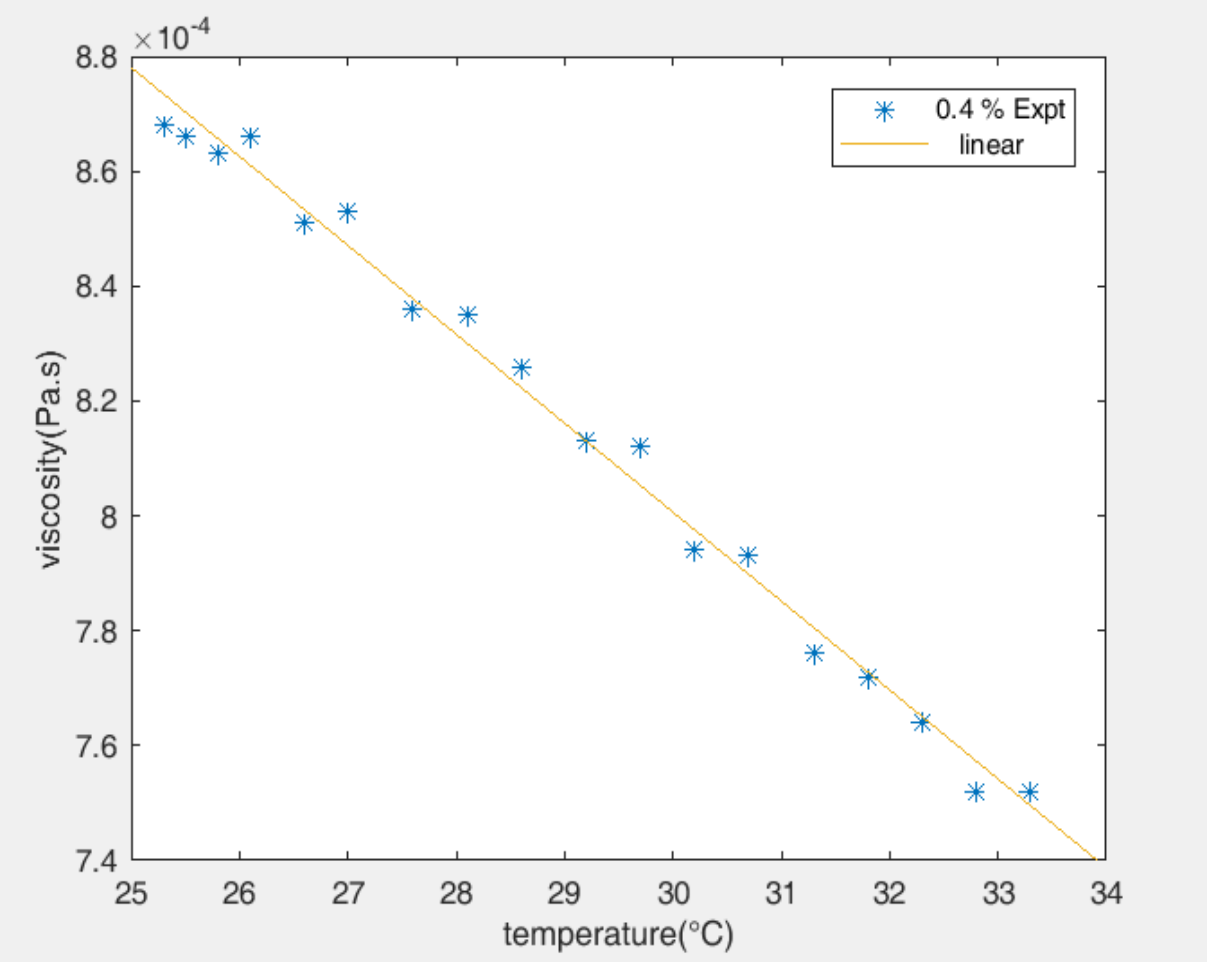

Figure 21 Proposed linear model by the experimental data of dynamic viscosity with respect to temperature in 0.4 vol.% concentration

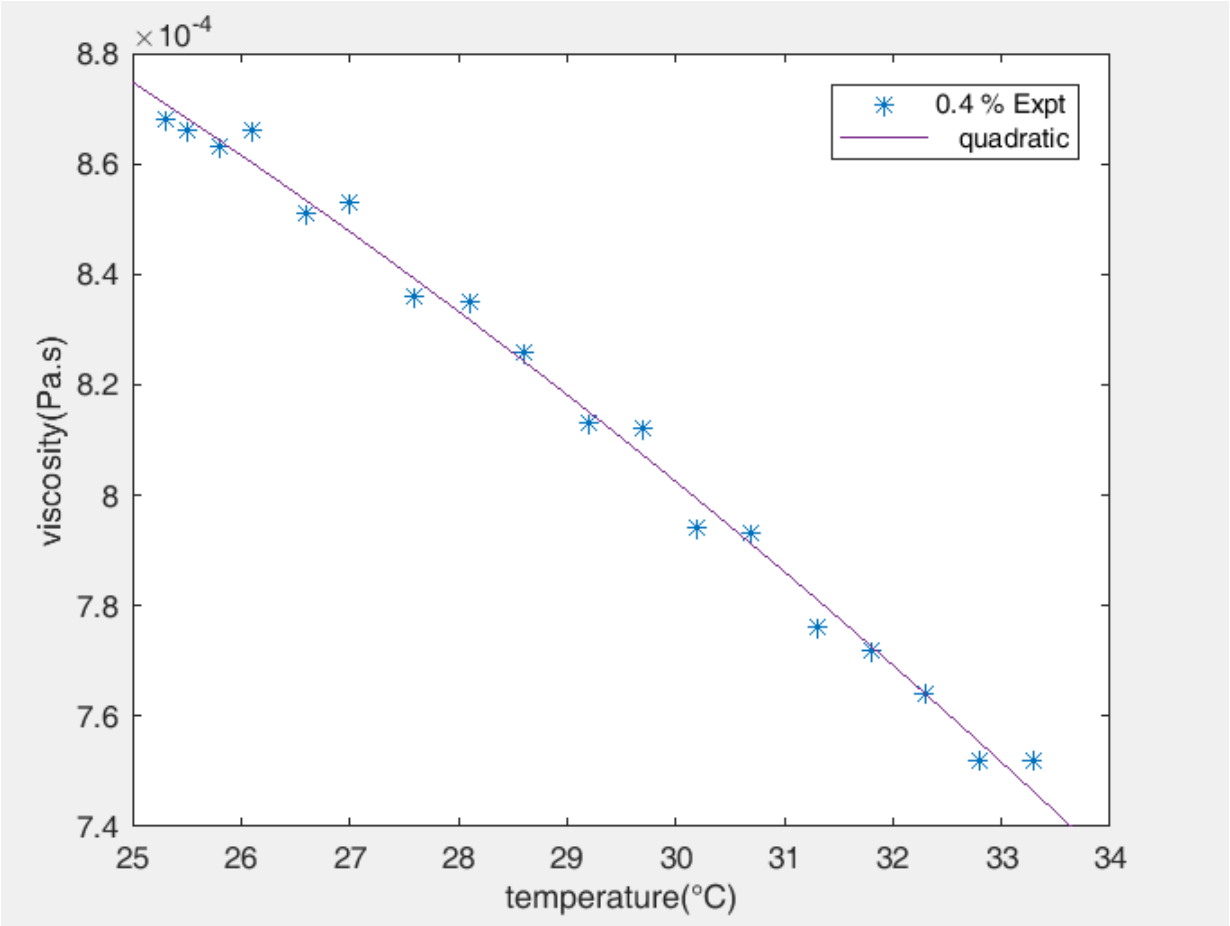

Figure 22 Proposed quadratic model by the experimental data of dynamic viscosity with respect to temperature in 0.4 vol.% concentration

Table 20 The dynamic viscosity ratio of nanofluid by increasing the concentration at 25.3°C

φ (vol. %)	$\frac{\mu_{nf}}{\mu_f}$
0.1	1.031515
0.2	1.031515
0.3	1.048484
0.4	1.052121

The sixth experiment: This experiment has been done for nanofluid at 27.6°C in different concentrations as it's presented in Table (21). Proposed quadratic model by the experimental data of dynamic viscosity by increasing the concentration at 27.6°C has been presented in Figure (24).

$$\frac{\mu_{nf}}{\mu_f} = 2.9\varphi^3 - 2\varphi^2 - 0.43\varphi + 1 \quad (21)$$

The seventh experiment: This experiment has been done for nanofluid at 30.7°C in different concentrations as it's presented in Table (22). Proposed quadratic model by the experimental data of dynamic viscosity by increasing the concentration at 30.7°C has been presented in Figure (25).

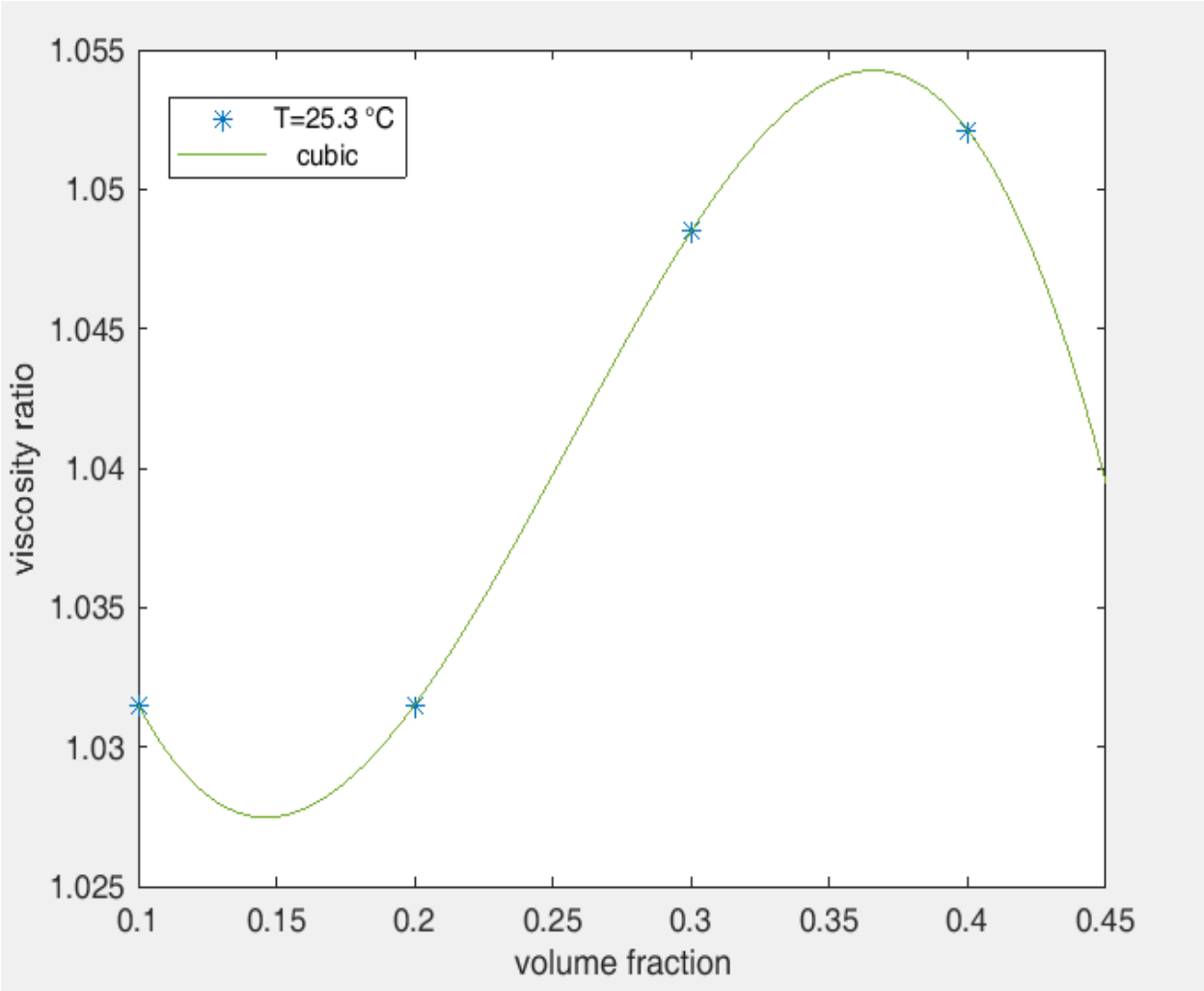

Figure 23 Proposed cubic model by the experimental data of dynamic viscosity by increasing the concentration at 25.3°C

Table 21 The dynamic viscosity ratio of nanofluid by increasing the concentration at 27.6°C

φ (vol. %)	$\frac{\mu_{nf}}{\mu_f}$
0.1	1.031486
0.2	1.036523
0.3	1.037783
0.4	1.052896

Table 22 The dynamic viscosity ratio of nanofluid by increasing the concentration at 30.7°C

φ(vol. %)	$\frac{\mu_{nf}}{\mu_f}$
0.1	1.030625
0.2	1.035952
0.3	1.042609
0.4	1.055925

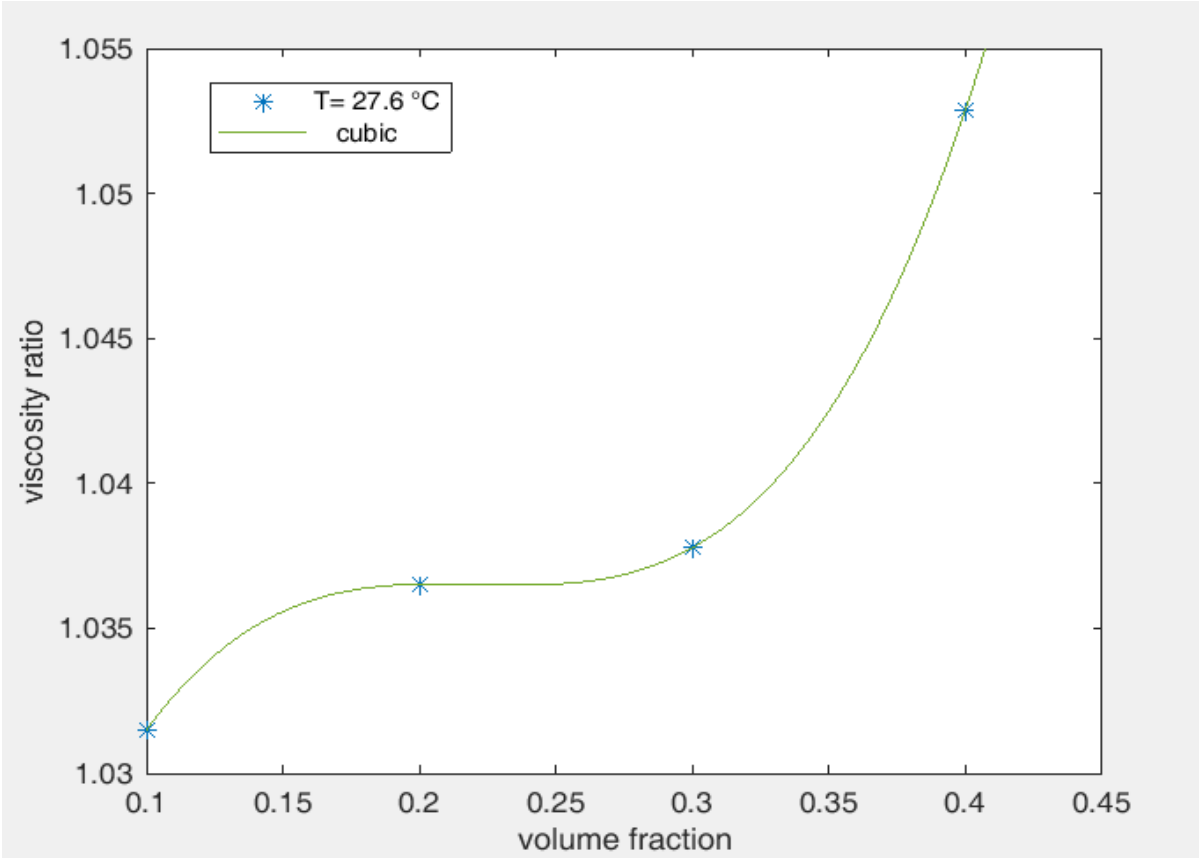

Figure 24 Proposed cubic model by the experimental data of dynamic viscosity by increasing the concentration at 27.6°C

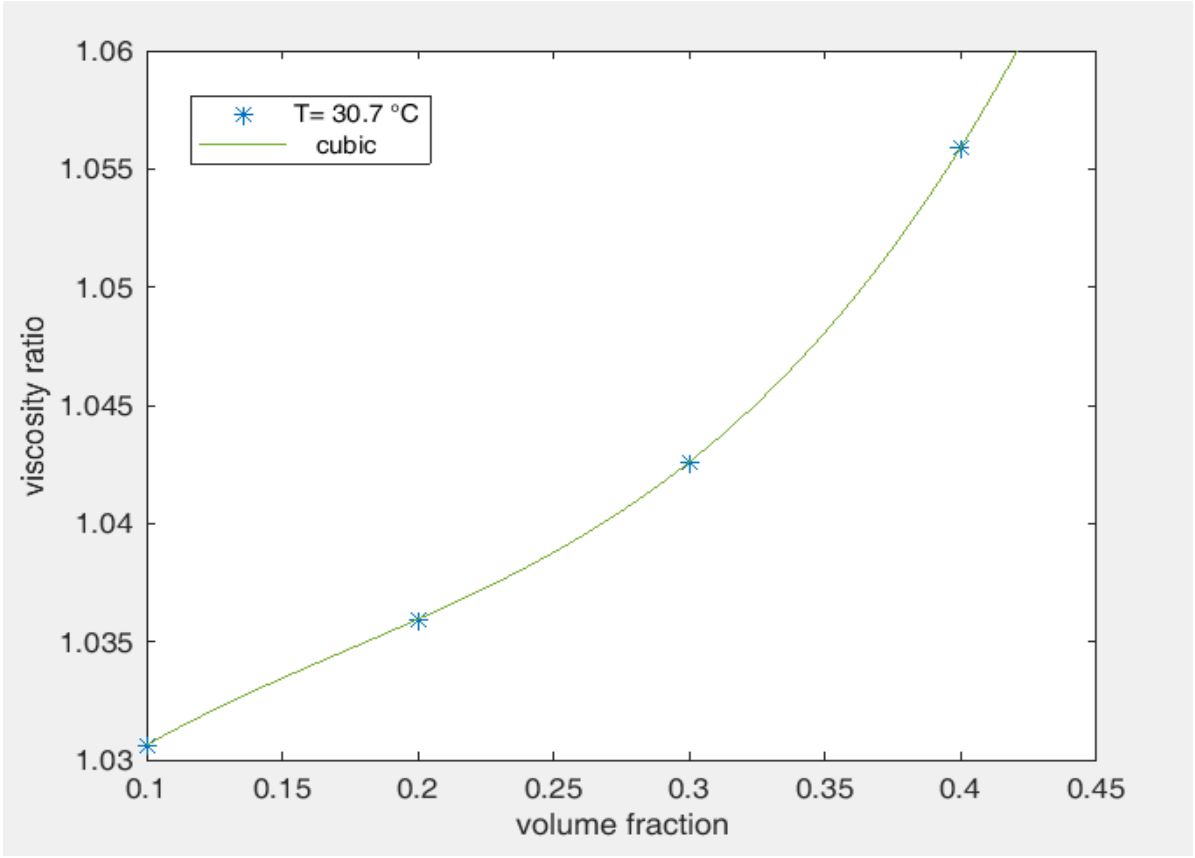

Figure 25 Proposed cubic model by the experimental data of dynamic viscosity by increasing the concentration at 30.7°C

Table 23 The dynamic viscosity ratio of nanofluid by increasing the concentration at 33.3°C

φ (vol. %)	$\frac{\mu_{nf}}{\mu_f}$
0.1	1.030942
0.2	1.037974
0.3	1.042194
0.4	1.057665

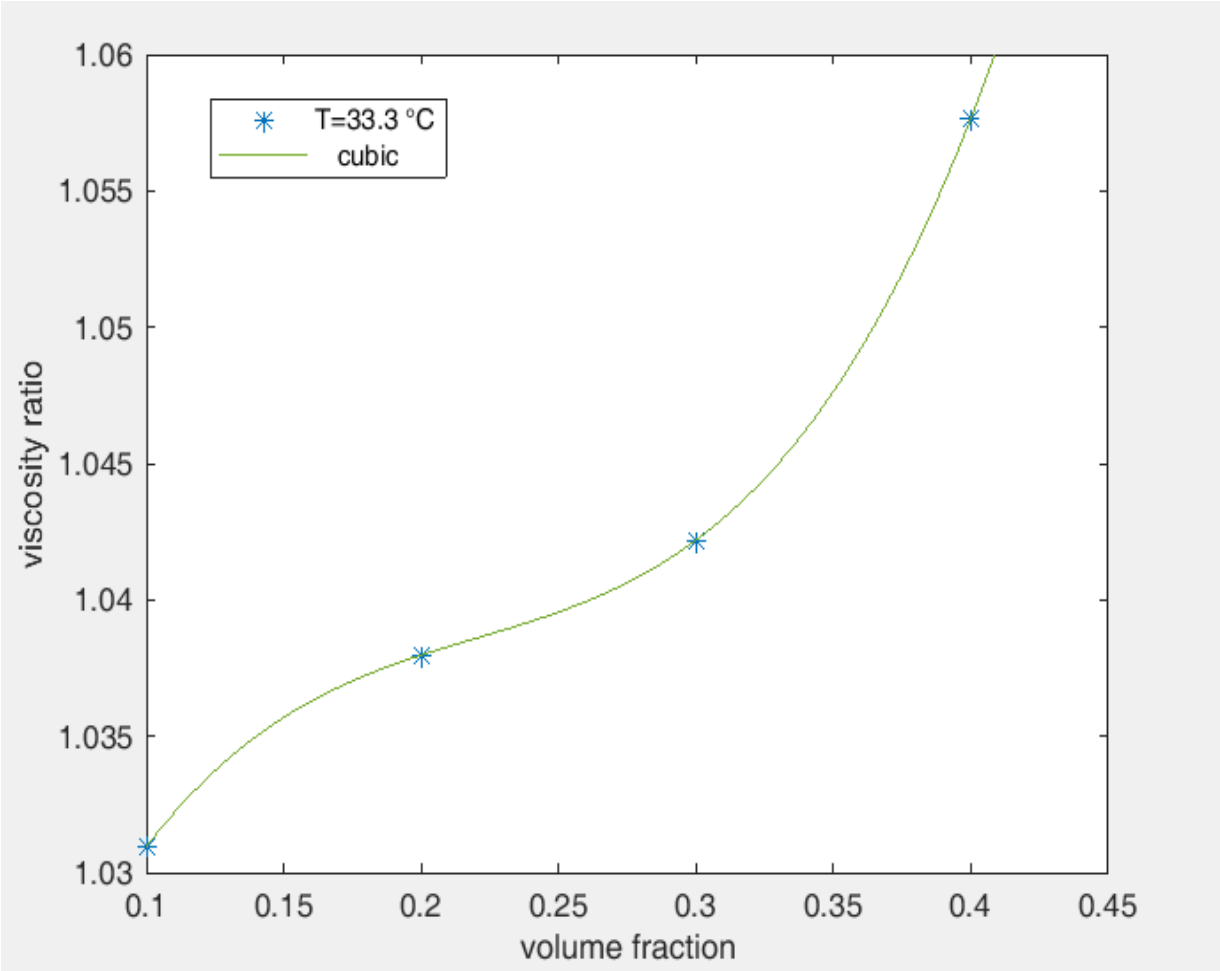

Figure 26 Proposed cubic model by the experimental data of dynamic viscosity by increasing the concentration at 33.3°C

$$\frac{\mu_{nf}}{\mu_f} = 0.89\varphi^3 - 0.47\varphi^2 + 0.13\varphi + 1 \tag{22}$$

The eighth experiment: This experiment has been done for nanofluid at 33.3°C in different concentrations as it's presented in Table (23). Proposed quadratic model by the experimental data of dynamic viscosity by increasing the concentration at 33.3°C has been presented in Figure (26).

$$\frac{\mu_{nf}}{\mu_f} = 2.3\varphi^3 - 1.5\varphi^2 + 0.37\varphi + 1 \tag{23}$$

3 Results and discussion

Effect of concentration on nanofluids thermal conductivity: As it's shown in Figure (27), the thermal conductivity at the beginning of the experiment for the volume fraction concentration of 0.1% was equal to 0.55 w/m.K, and for the volume fractions of 0.2% and 0.3% and 0.04% have been achieved 0.59, 0.63 and 0.65 w/m.K, respectively. Therefore, by the higher volume fractions, also the thermal conductivity have been more increased. On the other hand, by increasing the temperature, the thermal conductivity has been also increased.

Effect of temperature on thermal conductivity of nanofluid: As shown in Figure (28), the thermal conductivity ratio of the nanofluid to the base fluid at the beginning of the experiments in 25 °C has been equal to 1.037 w/m.K, which for the temperatures of 30, 35 and 40 °C have been achieved to 1.071, 1.084 and 1.107 w/m.K, respectively. Therefore, by the higher temperature, also the thermal conductivity of nanofluids have been more increased. Also, with the increase in volume fraction of nanoparticles, the thermal conductivity of nanofluids has increased.

Effect of nanoparticle volume fraction on the dynamic viscosity of nanofluid: As shown in Figure (29), the dynamic viscosity of the nanofluid to the base fluid at the beginning of the experiments for the volume fraction of 0.1% has been equal to 8.51×10^{-4}Pa.s, which for the volume fraction of 0.2%, 0.3% and 0.04%, have been obtained 8.51×10^{-4}, 8.65×10^{-4} and 8.68×10^{-4} Pa.s, respectively. Therefore, by the higher volume fraction concentrations, also the dynamic viscosity of nanofluids have been increased. Also, by increasing the temperature and the dynamic viscosity of nanofluids have been decreased.

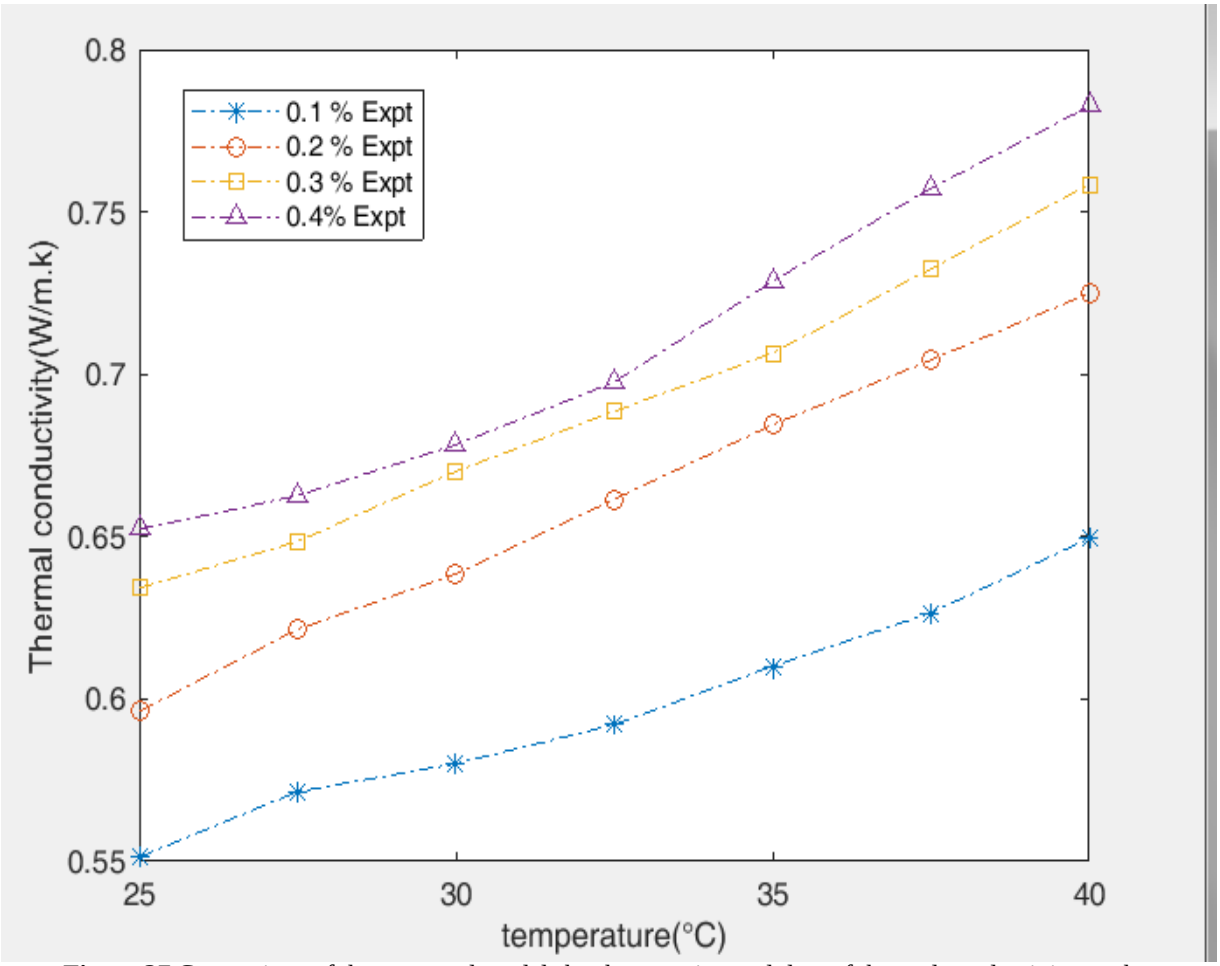

Figure 27 Comparison of the proposed models by the experimental data of thermal conductivity on the temperature at different volume fractions

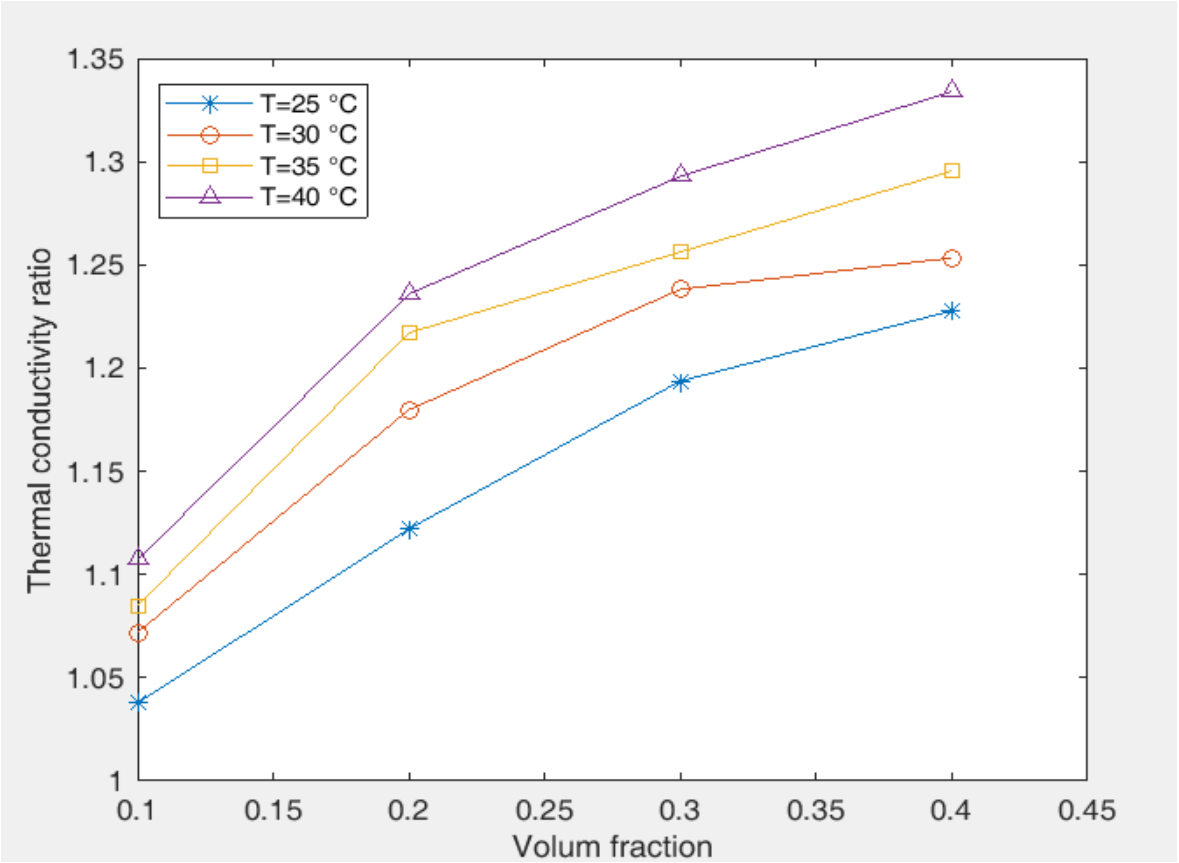

Figure 28 Comparison of the proposed models by the experimental data of thermal conductivity ratio on the volume fraction at different temperature

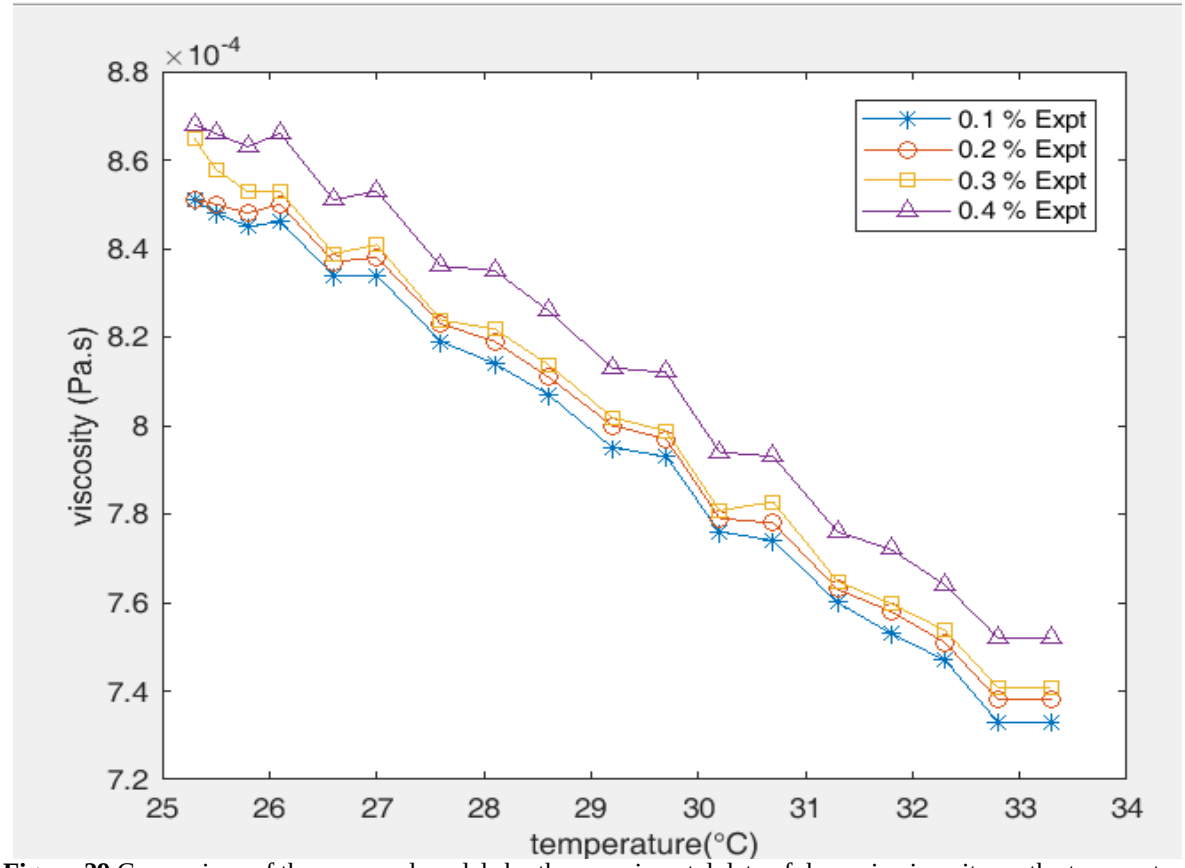

Figure 29 Comparison of the proposed models by the experimental data of dynamic viscosity on the temperature at different volume fraction

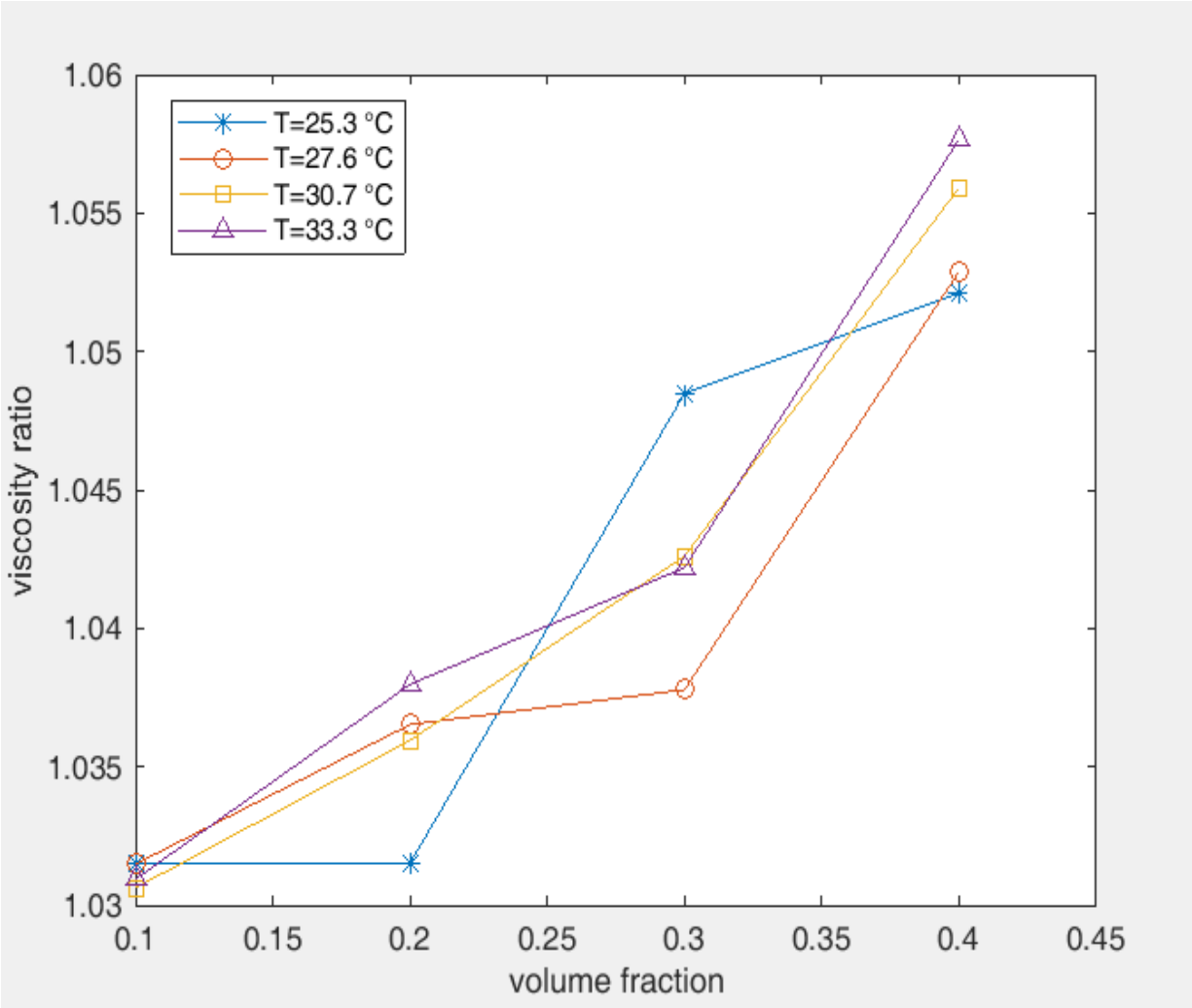

Figure 30 Comparison of the proposed models by the experimental data of dynamic viscosity ratio on the volume fraction at different temperature

Effect of temperature on dynamic viscosity of nanofluid: As shown in Figure (30), the dynamic viscosity ratio of the nanofluid to the base fluid by increasing the volume fraction concentration have been increased. However, but the dynamic viscosity ratio by increasing the temperature, in some cases only a slight increase has been observed, and in other cases, the dynamic viscosity ratio has been decreased.

4 Quality loss function by Taguchi method

Here and in this research, the value of response has considered the thermal conductivity and the dynamic viscosity of nanofluid, therefore, the main objectives have been included to maximize and minimize the response factors, respectively. And this ratio has determined by using the following relations:

Smaller–the better: Here, the quality characteristic is continuous and non-negative. It can take any value between 0 – ∞. The desired value (the target) is zero. These problems are characterized by the absence of scaling factor for examples: surface roughness, pollution, tire wear, etc. The S/N ratio is given by [28]:

$$\mathrm{S/N} = -10 \log \left[\frac{1}{n} \sum_{i=1}^{n} Y_i^2 \right] \tag{24}$$

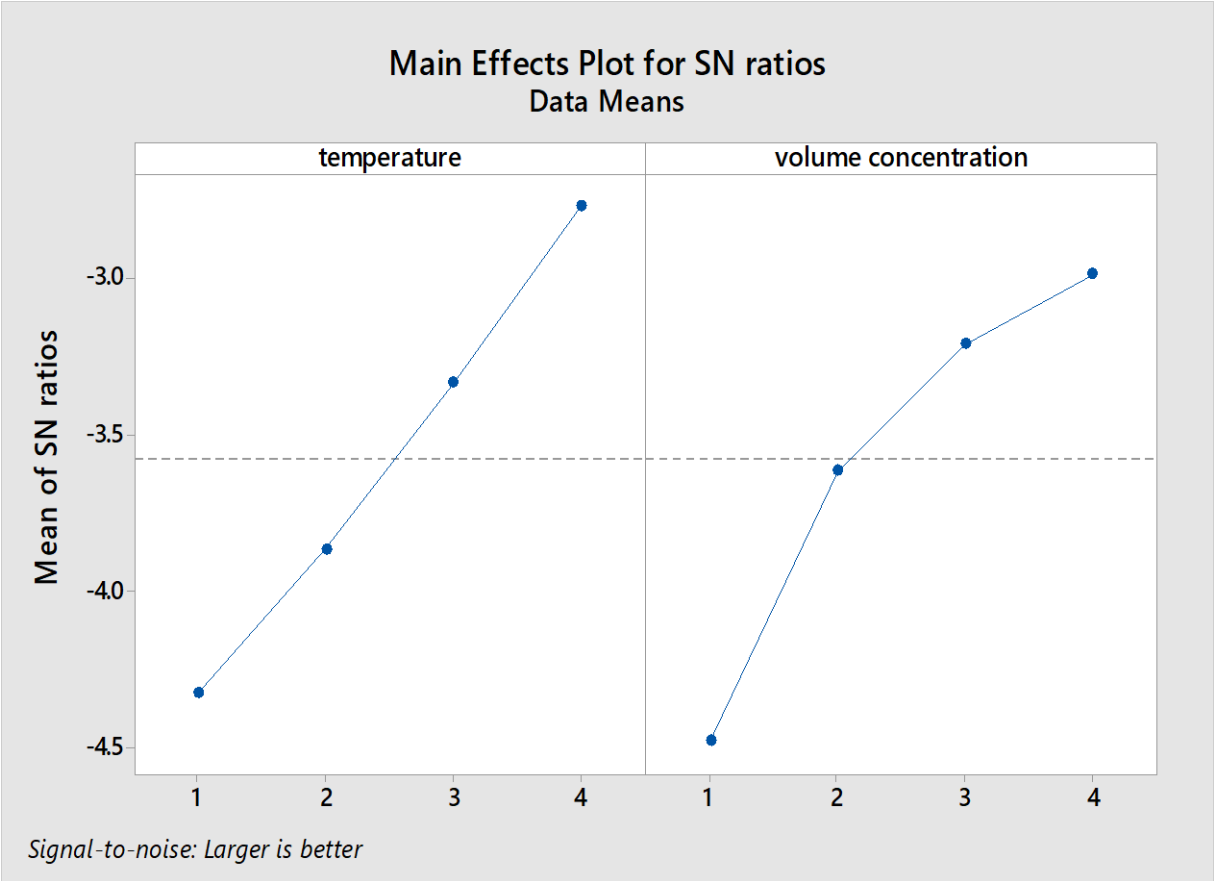

Figure 31 The mean signal-to-noise ratio in related levels and factors for nanofluid thermal conductivity

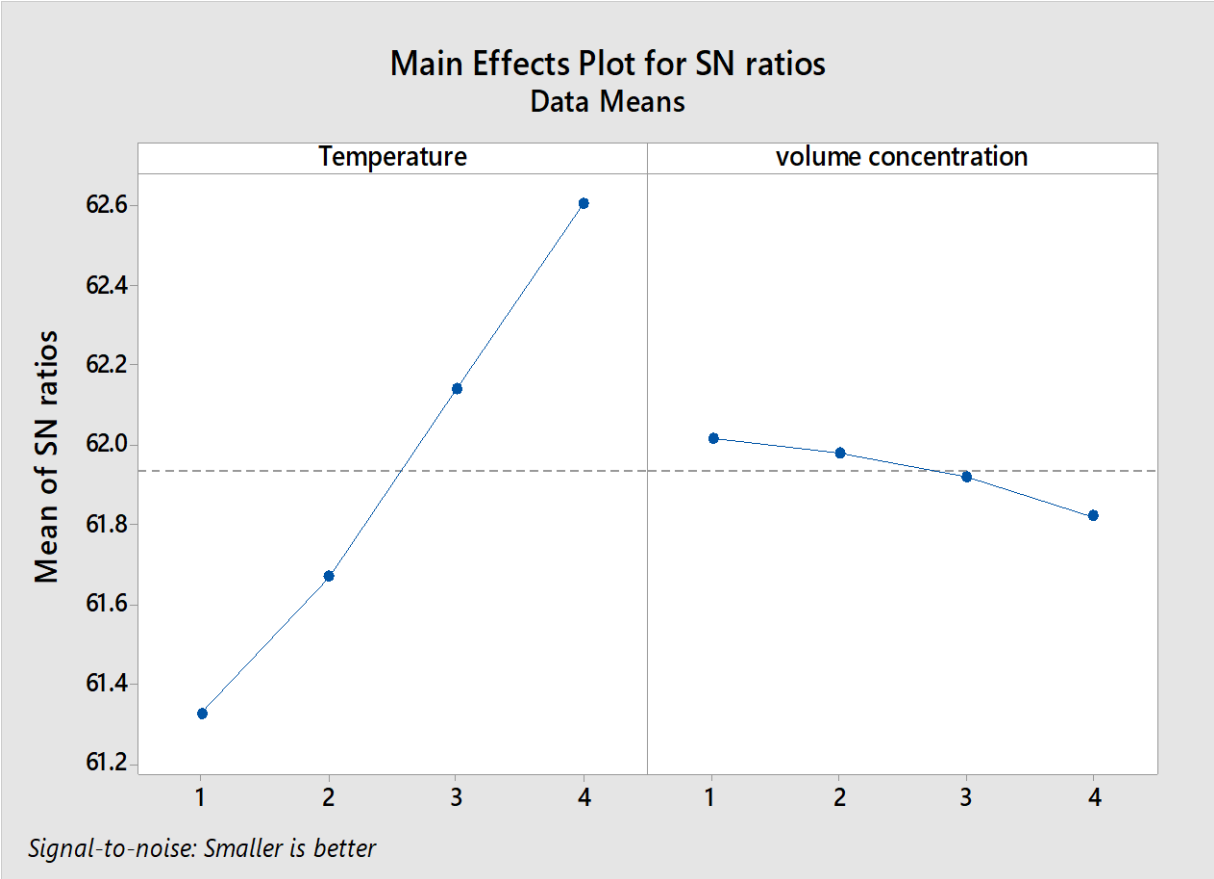

Figure 32 The mean signal-to-noise ratio in related levels and factors for nanofluid dynamic viscosity

Larger–the better: The quality characteristic is continuous and non-negative. It can take any value from 0 – ∞. The ideal target value of this type quality characteristic is ∞ (as large as possible). Quality characteristics like strength values, fuel efficiency, etc. are examples of this type. In these problems, there is no scaling factor. The S/N ratio is given by [42]:

$$S/N = -10 \log\left[\frac{1}{n}\sum_{i=1}^{n}\frac{1}{Y_i^2}\right] \quad (25)$$

In this relations, Y is the measured response value for each experiment where *n* is the number of replications. In fact, the signal to noise ratio or S/N ratio is a statistic that combines the mean and variance. Therefore, the optimization is a two-step process. First we select control factor levels corresponding to maximum signal to noise ratio, which minimizes noise. The higher signal to noise ratio, the higher thermal conductivity and the lower dynamic viscosity have been achieved. Therefore, it has been ensured that the effect of noise factors compared to the effect of main factors have been minimized. Thus, the final response has been had the lowest sensitivity to uncontrollable factors. The graphs of mean signal-to-noise ratio related to the two main factors at four levels have been shown in Figure (31) and Figure (32).

5 Conclusion

According to Figure (31), the signal-to-noise ratio in the main factor of nanofluid thermal conductivity has been increased by increasing temperature and volume fraction. Because of the signal-to-noise ratio has calculated from the ***Larger–the better*** relationship, therefore, it has be concluded that the thermal conductivity of nanofluid is higher at higher volume fractions and temperatures. Finally, in this condition, volume fraction of 0.4% and temperature of 40°C will be more suitable.
According to Figure (32), the signal-to-noise ratio in the main factor of nanofluid dynamic viscosity has been increased by increasing temperature and has been decreased by increasing volume fraction. Because of the signal-to-noise ratio has calculated from the ***smaller-the better*** relationship, therefore, it has be concluded that the dynamic viscosity of nanofluid is lower at lower volume fractions and higher temperature. Finally, in this condition, the volume fraction of 0.1% and the temperature of 33.3°C will be more suitable.

Acknowledgment

This study has been conducted based on a research grant No. 571393002 in the Materials and Energy Research Center (MERC), which is hereby appreciated.

References

[1] J. I. Prado, U. Calviño, and L. Lugo, "Experimental Methodology to Determine Thermal Conductivity of Nanofluids by using a Commercial Transient Hot-wire Device," *Applied Sciences,* Vol. 12, No. 1, p. 329, 2021, doi: https://doi.org/10.3390/app12010329.

[2] M. J. Assael, K. D. Antoniadis, and W. A. Wakeham, "Historical Evolution of the Transient Hot-wire Technique," *International Journal of Thermophysics,* Vol. 31, pp. 1051-1072, 2010, doi: https://link.springer.com/article/10.1007/s10765-010-0814-9.

[3] C. A. Nieto de Castro and M. J. V. Lourenço, "Towards the Correct Measurement of Thermal Conductivity of Ionic Melts and Nanofluids," *Energies*, Vol. 13, No. 1, p. 99, 2019, doi: http://doi.org/10.3390/en13010099.

[4] A. Palacios, L. Cong, M. Navarro, Y. Ding, and C. Barreneche, "Thermal Conductivity Measurement Techniques for Characterizing Thermal Energy Storage Materials–A Review," *Renewable and Sustainable Energy Reviews*, Vol. 108, PP. 32-52, 2019, doi: https://linkinghub.elsevier.com/retrieve/pii/S1364032119301625.

[5] N. Karthikeyan, J. Philip, and B. Raj, "Effect of Clustering on the Thermal Conductivity of Nanofluids," *Materials Chemistry and Physics*, Vol. 109, No. 1, pp. 50-55, 2008, doi: https://doi.org/10.1016/j.matchemphys.2007.10.029.

[6] R. R. Riehl and S. Mancin, "Estimation of Thermophysical Properties for Accurate Numerical Simulation of Nanofluid Heat Transfer Applied to a Loop Heat Pipe," *International Journal of Thermofluids*, Vol. 14, p. 100158, 2022, doi: https://doi.org/10.1016/j.ijft.2022.100158.

[7] H. Chen, Y. Ding, and C. Tan, "Rheological Behaviour of Nanofluids," *New Journal of Physics*, Vol. 9, No. 10, p. 367, 2007, doi: https://iopscience.iop.org/article/10.1088/1367-2630/9/10/367/meta.

[8] G. Paul, M. Chopkar, I. Manna, and P. Das, "Techniques for Measuring the Thermal Conductivity of Nanofluids: A Review," *Renewable and Sustainable Energy Reviews*, Vol. 14, No. 7,PP. 1913-1924, 2010, doi: https://doi.org/10.1016/j.rser.2010.03.017.

[9] X. Wang, X. Xu, and S. U. Choi, "Thermal Conductivity of Nanoparticle-fluid Mixture," *Journal of Thermophysics and Heat Transfer*, Vol. 13, No. 4, pp. 474-480, 1999, doi: http://dx.doi.org/10.2514/2.6486.

[10] Y. Xuan and Q. Li, "Heat Transfer Enhancement of Nanofluids," *International Journal of Heat and Fluid Flow*, Vol. 21, No. 1, pp. 58-64, 2000, doi: https://doi.org/10.1016/S0142-727X(99)00067-3.

[11] S. Choi, Z. G. Zhang, W. Yu, F. Lockwood, and E. Grulke, "Anomalous Thermal Conductivity Enhancement in Nanotube Suspensions," *Applied Physics Letters*, Vol. 79, No. 14, pp. 2252-2254, 2001, doi: http://dx.doi.org/10.1063/1.1408272.

[12] C. H. Li and G. Peterson, "Experimental Investigation of Temperature and Volume Fraction Variations on the Effective Thermal Conductivity of Nanoparticle Suspensions Nanofluids)," *Journal of Applied Physics*, Vol. 99, No. 8, 2006. doi:https://doi.org/10.1063/1.2191571.

[13] S. Murshed, K. Leong, and C. Yang, "Enhanced Thermal Conductivity of TiO2—Water Based Nanofluids," *International Journal of Thermal Sciences*, Vol. 44, No. 4, pp. 367-373, 2005, doi: https://doi.org/10.1016/j.ijthermalsci.2004.12.005.

[14] D.-H. Yoo, K. Hong, and H.-S. Yang, "Study of Thermal Conductivity of Nanofluids for the Application of Heat Transfer Fluids," *Thermochimica Acta*, Vol. 455, No. 1-2, pp. 66-69, 2007, doi: https://doi.org/10.1016/j.tca.2006.12.006.

[15] D. Wen and Y. Ding, "Formulation of Nanofluids for Natural Convective Heat Transfer Applications," *International Journal of Heat and Fluid Flow*, Vol. 26, No. 6, pp. 855-864, 2005, doi: https://doi.org/10.1016/j.ijheatfluidflow.2005.10.005.

[16] H. Chen, Y. Ding, Y. He, and C. Tan, "Rheological Behaviour of Ethylene Glycol Based Titania Nanofluids," *Chemical Physics Letters*, Vol. 444, No. 4-6, pp. 333-337, 2007, doi: https://doi.org/10.1016/j.cplett.2007.07.046.

[17] S. Murshed, K. Leong, and C. Yang, "Investigations of Thermal Conductivity and Viscosity of Nanofluids," *International Journal of Thermal Sciences*, Vol. 47, No. 5, pp. 560-568, 2008, doi: https://doi.org/10.1016/j.ijthermalsci.2007.05.004.

[18] J. Philip and P. D. Shima, "Thermal Properties of Nanofluids," *Advances in Colloid and Interface Science*, Vol. 183, pp. 30-45, 2012, doi: http://doi.org/10.1016/j.cis.2012.08.001.

[19] X.-j. Wang and D.-s. Zhu, "Investigation of pH and SDBS on Enhancement of Thermal Conductivity in Nanofluids," *Chemical Physics Letters*, Vol. 470, No. 1-3, pp. 107-111, 2009, doi: http://doi.org/10.1016/j.cplett.2009.01.035.

[20] P. K. Das, "A Review Based on the Effect and Mechanism of Thermal Conductivity of Normal Nanofluids and Hybrid Nanofluids," *Journal of Molecular Liquids*, Vol. 240, pp. 420-446, 2017, doi: https://doi.org/10.1016/j.molliq.2017.05.071.

[21] B. Buonomo, O. Manca, L. Marinelli, and S. Nardini, "Effect of Temperature and Sonication Time on Nanofluid Thermal Conductivity Measurements by Nano-flash Method," *Applied Thermal Engineering*, Vol. 91, pp. 181-190, 2015, doi: https://doi.org/10.1016/j.applthermaleng.2015.07.077.

[22] I. Mahbubul, I. Shahrul, S. Khaleduzzaman, R. Saidur, M. Amalina, and A. Turgut, "Experimental Investigation on Effect of Ultrasonication Duration on Colloidal Dispersion and Thermophysical Properties of Alumina–water Nanofluid," *International Journal of Heat and Mass Transfer*, Vol. 88, pp. 73-81, 2015, doi: https://doi.org/10.1016/j.ijheatmasstransfer.2015.04.048.

[23] B. Lamas, B. Abreu, A. Fonseca, N. Martins, and M. Oliveira, "Critical Analysis of the Thermal Conductivity Models for CNT Based Nanofluids," *International Journal of Thermal Sciences*, Vol. 78, pp. 65-76, 2014, doi: https://doi.org/10.1016/j.ijthermalsci.2013.11.017.

[24] Y. S. Ju, J. Kim, and M.-T. Hung, "Experimental Study of Heat Conduction in Aqueous Suspensions of Aluminum Oxide Nanoparticles," 2008, doi: https://doi.org/10.1115/1.2945886.

[25] M. Kole and T. Dey, "Effect of Prolonged Ultrasonication on the Thermal Conductivity of ZnO–Ethylene Glycol Nanofluids," *Thermochimica Acta*, Vol. 535, pp. 58-65, 2012, doi: https://doi.org/10.1016/j.tca.2012.02.016.

[26] J.-C. Yang, F.-C. Li, W.-W. Zhou, Y.-R. He, and B.-C. Jiang, "Experimental Investigation on the Thermal Conductivity and Shear Viscosity of Viscoelastic-fluid-based

Nanofluids," *International Journal of Heat and Mass Transfer,* Vol. 55, No. 11-12, pp. 3160-3166, 2012, doi: https://doi.org/10.1016/j.ijheatmasstransfer.2012.02.052.

[27] H. Xie, M. Fujii, and X. Zhang, "Effect of Interfacial Nanolayer on the Effective Thermal Conductivity of Nanoparticle-fluid Mixture," *International Journal of Heat and Mass Transfer,* Vol. 48, No. 14, pp. 2926-2932, 2005, doi: https://doi.org/10.1016/j.ijheatmasstransfer.2004.10.040.

[28] J. Avsec and M. Oblak, "The Calculation of Thermal Conductivity, Viscosity and Thermodynamic Properties for Nanofluids on the Basis of Statistical Nanomechanics," *International Journal of Heat and Mass Transfer,* Vol. 50, No. 21-22, pp. 4331-4341, 2007, doi: https://doi.org/10.1016/j.ijheatmasstransfer.2007.01.064.

[29] B. C. Pak and Y. I. Cho, "Hydrodynamic and Heat Transfer Study of Dispersed Fluids with Submicron Metallic Oxide Particles," *Experimental Heat Transfer an International Journal,* Vol. 11, No. 2, pp. 151-170, 1998, doi: https://doi.org/10.1080/08916159808946559.

[30] W. Yu and S. Choi, "The Role of Interfacial Layers in the Enhanced Thermal Conductivity of Nanofluids: A Renovated Maxwell Model," *Journal of Nanoparticle Research,* Vol. 5, pp. 167-171, 2003, doi: https://doi.org/10.1023/A:1024438603801.

[31] S. Mirian, G. Ansarifar, and M. Esteki, "Nanofluid Applications in Pressurized Water Reactors: A Review," *International Journal of Energy Research,* Vol. 46, No. 15, pp. 22314-22335, 2022, doi: https://doi.org/10.1002/er.8681.

[32] M. Chandrasekar, S. Suresh, R. Srinivasan, and A. C. Bose, "New Analytical Models to Investigate Thermal Conductivity of Nanofluids," *Journal of Nanoscience and Nanotechnology,* Vol. 9, No. 1, pp. 533-538, 2009, doi: https://doi.org/10.1166/jnn.2009.J025.

[33] M. Corcione, "Empirical Correlating Equations for Predicting the Effective Thermal Conductivity and Dynamic Viscosity of Nanofluids," *Energy Conversion and Management,* Vol. 52, No. 1, pp. 789-793, 2011, doi: https://doi.org/10.1016/j.enconman.2010.06.072.

[34] [1] P. K. Das, "A Review Based on the Effect and Mechanism of Thermal Conductivity of Normal Nanofluids and Hybrid Nanofluids," *Journal of Molecular Liquids,* Vol. 240, pp. 420-446, 2017, doi: https://doi.org/10.1016/j.molliq.2017.05.071.

[35] B. Buonomo, O. Manca, L. Marinelli, and S. Nardini, "Effect of Temperature and Sonication Time on Nanofluid Thermal Conductivity Measurements by Nano-flash Method," *Applied Thermal Engineering,* Vol. 91, pp. 181-190, 2015, doi: https://doi.org/10.1016/j.applthermaleng.2015.07.077.

[36] I. Mahbubul, I. Shahrul, S. Khaleduzzaman, R. Saidur, M. Amalina, and A. Turgut, "Experimental Investigation on Effect of Ultrasonication Duration on Colloidal Dispersion and Thermophysical Properties of Alumina–water Nanofluid," *International Journal of Heat and Mass Transfer,* Vol. 88, pp. 73-81, 2015, doi: https://doi.org/10.1016/j.ijheatmasstransfer.2015.04.048.

[37] B. Lamas, B. Abreu, A. Fonseca, N. Martins, and M. Oliveira, "Critical Analysis of the Thermal Conductivity Models for CNT Based Nanofluids," *International Journal of*

Thermal Sciences, Vol. 78, pp. 65-76, 2014, doi: https://doi.org/10.1016/j.ijthermalsci.2013.11.017.

[38] Y. S. Ju, J. Kim, and M.-T. Hung, "Experimental Study of Heat Conduction in Aqueous Suspensions of Aluminum Oxide Nanoparticles," 2008, doi: https://doi.org/10.1115/1.2945886.

[39] M. Kole and T. Dey, "Effect of Prolonged Ultrasonication on the Thermal Conductivity of ZnO–ethylene Glycol Nanofluids," *Thermochimica Acta*, Vol. 535, pp. 58-65, 2012, doi: https://doi.org/10.1016/j.tca.2012.02.016.

[40] J.-C. Yang, F.-C. Li, W.-W. Zhou, Y.-R. He, and B.-C. Jiang, "Experimental Investigation on the Thermal Conductivity and Shear Viscosity of Viscoelastic-fluid-based Nanofluids," *International Journal of Heat and Mass Transfer*, Vol. 55, No. 11-12, pp. 3160-3166, 2012, doi: https://doi.org/10.1016/j.ijheatmasstransfer.2012.02.052.

[41] T.-K. Hong, H.-S. Yang, and C. Choi, "Study of the Enhanced Thermal Conductivity of Fe Nanofluids," *Journal of Applied Physics*, Vol. 97, No. 6, 2005, doi: https://doi.org/10.1063/1.1861145.

[42] [1] K. Krishnaiah and P. Shahabudeen, *Applied Design of Experiments and Taguchi Methods*. PHI Learning Pvt. Ltd., 2012, https://eko.staff.uns.ac.id/files/2014/09/Buku-Alternatif.pdf.